

Review

## Connectivity analyses for task-based fMRI



Shenyang Huang <sup>a,b,\*</sup>, Felipe De Brigard <sup>a,b,c</sup>, Roberto Cabeza <sup>a,b</sup>,  
Simon W. Davis <sup>a,c,d</sup>

<sup>a</sup> Department of Psychology and Neuroscience, Duke University, Durham, NC 27708, United States

<sup>b</sup> Center for Cognitive Neuroscience, Duke University, Durham, NC 27708, United States

<sup>c</sup> Department of Philosophy, Duke University, Durham, NC 27708, United States

<sup>d</sup> Department of Neurology, Duke University School of Medicine, Durham, NC 27708, United States

ARTICLE INFO

Keywords:

fMRI

Functional connectivity

Multivariate pattern analysis

Representational similarity analysis

Graph theory

ABSTRACT

Functional connectivity is conventionally defined by measuring the similarity between brain signals from two regions. The technique has become widely adopted in the analysis of functional magnetic resonance imaging (fMRI) data, where it has provided cognitive neuroscientists with abundant information on how brain regions interact to support complex cognition. However, in the past decade the notion of “connectivity” has expanded in both the complexity and heterogeneity of its application to cognitive neuroscience, resulting in greater difficulty of interpretation, replication, and cross-study comparisons. In this paper, we begin with the canonical notions of functional connectivity and then introduce recent methodological developments that either estimate some alternative form of connectivity or extend the analytical framework, with the hope of bringing better clarity for cognitive neuroscience researchers.

### 1. Introduction

An established tradition of cognitive neuroscience research has focused on functional localization: identifying specific brain regions that show high functional specificity to certain cognitive tasks [1]. For example, the fusiform gyrus has been linked to face recognition [2], and the parahippocampal gyrus has been linked to processing local spatial environments [3]. This approach has been very useful in mapping cortical specificity but is limited by the fact that the mapping between cognition and cortex is not bijective, and the cognitive operations of simple behaviors may require a complex mapping to spatially distributed areas. As a result, the brain is increasingly regarded as a large network with abundant connections among disparate brain regions (see Fig. 1) [4]. To investigate how those connections relate to behavior, researchers have employed a group of statistical methods commonly referred to as *functional connectivity*, quantifying the statistical—often linear—relationship between *univariate* activation levels of brain regions [5,6]. In recent years, others have developed alternative analytical frameworks that probe the degree to which different brain regions communicate informational contents represented in their multivariate neural patterns [7], which include techniques known as *informational* and *representational connectivity*. Unlike functional connectivity, these approaches seek to answer not *whether* two regions are communicating but *what* they are communicating about. Since the introduction of these methods, however, some have noted that the notion of “connectivity” is unpleasantly ambiguous and requires further clarification ([8,9]; cf. [10]). Different studies might characterize the statistical dependency between two brain regions under different assumptions or at different levels, yet both might refer to their results

\* Corresponding author.

E-mail address: [shenyang.huang@duke.edu](mailto:shenyang.huang@duke.edu) (S. Huang).

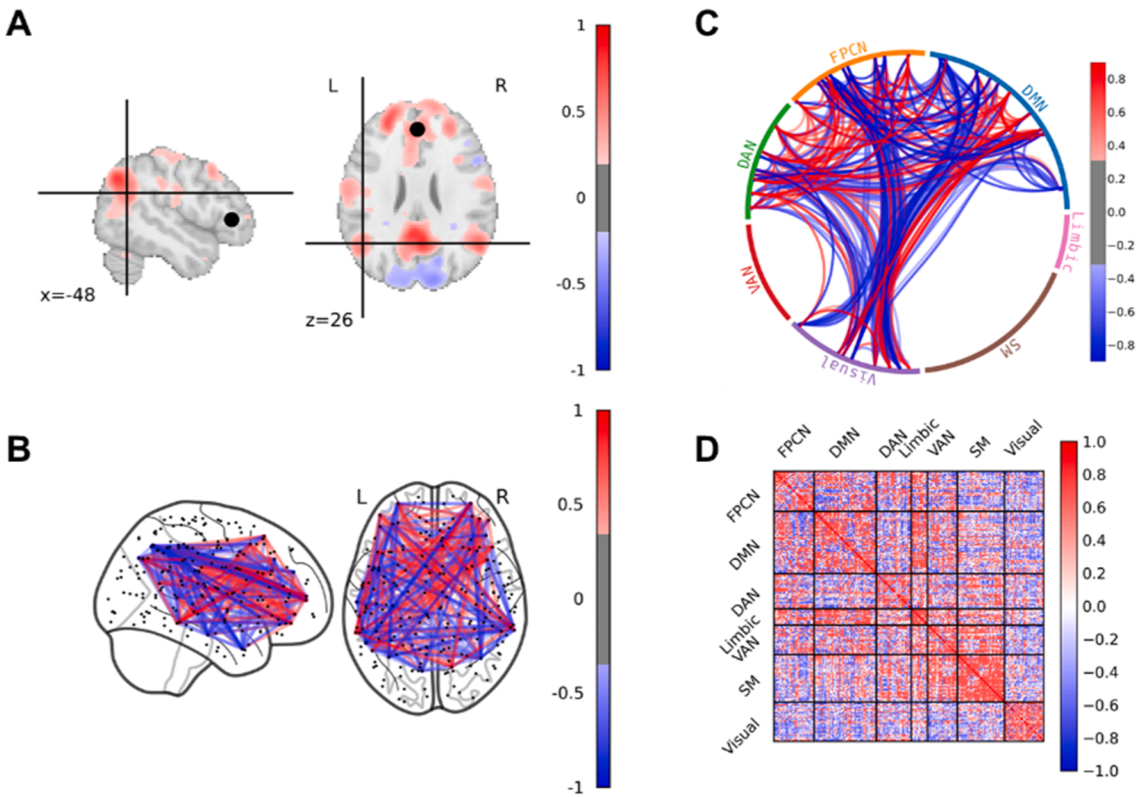


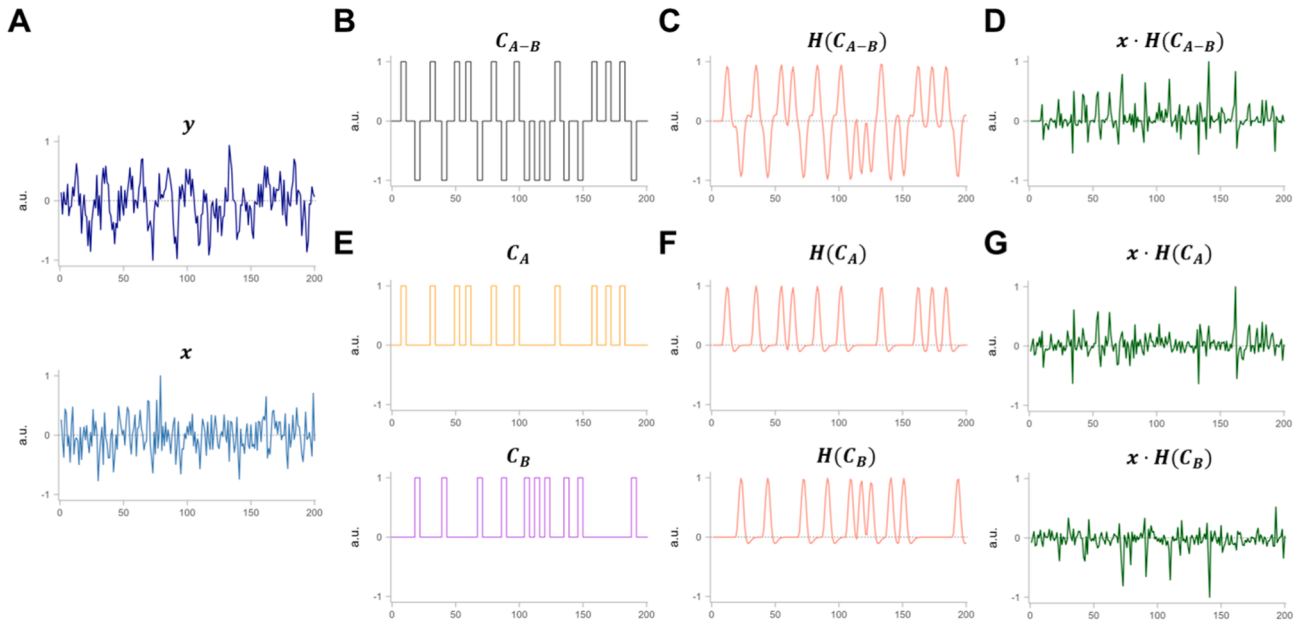
**Fig. 1.** Common visualizations of task fMRI-based brain connectivity. All visualizations were created using synthetic data. **A)** Statistic map of seed-based thresholded connectivity on anatomical brain slices, with the seed region (medial prefrontal cortex) indicated by the green circle. **B)** Graph representation of thresholded connections on glass brain slices, with dots indicating the center of regions of interests and edge colors reflecting connection strength. **C)** Chord diagram of the same connections shown in **(B)**. Networks were assigned based on the Schaefer 7network-and-200-parcel atlas [11]. **D)** Heatmap of the full connectivity matrix with cells color-coded to indicate connection strength. The following software programs were used to create these visualizations: **A** and **B**, Nilearn [12]. **C**, NiChord [13]. **D**, Matplotlib [14]. For a more comprehensive and detailed discussion on visualizations of brain networks of all kinds, readers are referred to [15].

as “functional connectivity”. This ambiguity hinders effective scientific communication of results and cross-study comparisons aiming at generalizability. To address these issues, this review aims to provide a detailed introduction to extant connectivity methods and their extensions that are commonly used in task-based functional magnetic resonance imaging (fMRI) paradigms.

## 2. Functional connectivity

Functional connectivity is defined as the covariation of separate brain regions in terms of some neurophysiological index [5]. In fMRI, the recorded neurophysiological index is the blood-oxygenation-level-dependent (BOLD) activity at a single voxel, and the voxel-wise BOLD signal time courses or time series may be averaged across voxels within a certain brain region (e.g., hippocampus) to obtain a regional BOLD time series. Then, the correlation of two BOLD time series from different sources (e.g., hippocampus and amygdala) is interpreted as their functional connectivity. This relatively straightforward approach is commonly implemented on resting-state fMRI data to quantify *resting-state* or *intrinsic* functional connectivity for individual participants [16,17].<sup>1</sup> Task-based fMRI paradigms typically bear more complexity than resting-state scans, as they consist of experimental cognitions designed to engage specific cognitive processes, such as memory, emotion, and decision-making. Two critical features of task-related paradigms are important to highlight and will be considered throughout this review: *event timing* and *conditional change*. First, an fMRI scan may include multiple task blocks or trials with jittered intervals, necessitating the time-locking of neural measures to events of interest. As such, task-related paradigms prioritize the concurrent *event timing* of the fMRI signal with the cognitive response and often make use of some theoretical model of hemodynamic responses. Second, researchers employing task-related fMRI are focused on how the same

<sup>1</sup> The availability of large-scale resting-state connectomes has driven efforts to derive a universal taxonomy of functional brain networks, that is, groups of brain regions that intimately connect to each other [18], which have facilitated clinical neuroimaging research [19]. However, controversies remain in the precise definitions and nomenclature of such networks [20].



$$\text{sPPI model: } y = \beta_0 + \beta_1 \cdot x + \beta_2 \cdot H(C_{A-B}) + \beta_3 x \cdot H(C_{A-B}) + \varepsilon$$

$$\text{gPPI model: } y = \beta_0 + \beta_1 \cdot x + \beta_2 \cdot H(C_A) + \beta_3 \cdot x \cdot H(C_A) + \beta_4 \cdot H(C_B) + \beta_5 \cdot x \cdot H(C_B) + \varepsilon$$

**Fig. 2.** Psychophysiological interaction (PPI) analysis. **A)** Physiological activity time courses from the target region ( $y$ ) and the seed region ( $x$ ). **B)** In standard PPI, a single task variable  $C_{A-B}$  codes the contrast condition A - condition B. **C)** The psychological variable  $H(C_{A-B})$  is the expected BOLD response according to the task, which is obtained by convolving the task variable with the hemodynamic response function. **D)** The PPI term is computed as the element-wise product of the seed physiological activity  $x$  and the psychological variable  $H(C_{A-B})$ . **E)** In generalized PPI, task conditions A and B are coded in separate task variables,  $C_A$  and  $C_B$ , which are then used to create **F)** two psychological variables,  $H(C_A)$  and  $H(C_B)$ , and subsequently **G)** two separate PPI terms.

participant performs, behaviorally and neurally, in different task conditions or events. In other words, the measure of interest is the *conditional change* in functional connectivity (or other related measures), rather than functional connectivity *per se*. Keeping these factors in mind, we review three common analytical frameworks of task-fMRI-based functional connectivity.

## 2.1. Psychophysiological interaction

One of the earliest and still most commonly used methods to examine how multi-region interplay supports cognition is psychophysiological interaction, or PPI. In its original formulation (now referred to as *standard* PPI or sPPI) [21], this approach characterizes the difference in two brain regions' functional connectivity during two conditions or cognitive states. In a nutshell, the sPPI approach fits a linear regression model,

$$y = \beta_0 + \beta_1 \cdot x + \beta_2 \cdot H(C) + \beta_3 \cdot x \cdot H(C) + \epsilon$$

where  $y$  and  $x$  are (neuro)physiological time courses (i.e., BOLD time series) of the target and seed brain regions, respectively.  $C$  is a psychological variable that reflects the experimental design and task timing (e.g., task on vs. off), and its convolution with the hemodynamic response function (HRF,  $H(\cdot)$ ) accounts for the delay in BOLD responses. The interaction term  $x \cdot H(C)$ , computed as the element-wise product of  $x$  and  $H(C)$ , is the variable of focal interest (see Fig. 2A-D). Nuisance regressors such as motion parameters and global signal could also be included as additional covariates.

The key parameter estimate from the sPPI model is  $\beta_3$ , which is the estimated weight of the interaction term, and it quantifies the extent to which the seed region changes its influence on the target region in different task conditions, i.e., task-modulated change in seed-to-target functional connectivity.<sup>2</sup> Once the regression coefficient  $\beta_3$  is obtained for each participant, subsequent tests are usually performed at the group level, such as a two-sample *t*-test that determines whether two cohorts differ in task-modulated connectivity change [22].

Since the original conceptualization of PPI, there have been three notable methodological developments. First, sPPI only supports the meaningful interpretation of one parametric modulation (which includes binary contrasts; see Fig. 2B), yet some researchers may wish to test more manipulations simultaneously (e.g., *condition A*, *condition B*, *condition C*, and *baseline*). An extension of PPI termed *generalized* PPI or gPPI [23] solved this limitation via an alternative formulation: instead of having just one psychological variable  $C$  that codes for all conditions or manipulation levels, gPPI would model each task condition as a separate psychological variable  $C_j$  (where  $1 = \text{condition } j$ ,  $0 = \text{all else}$ ), as well as computing separate interaction terms  $x \cdot H(C_j)$  (see Fig. 2E-G). This generalized formulation allows for the estimation of condition-specific functional connectivity during each task condition, which can be contrasted in subsequent tests. In addition, gPPI is found to outperform sPPI in terms of Type II errors, especially for event-related designs ([24, 25]; cf. [26]).

Second, originally PPI analyses of task-based fMRI data compute the interaction term simply as the element-wise product of seed region BOLD signal time course and the psychological variable—experimental design convolved with HRF; in other words, this interaction is modeled at the *hemodynamic* level. However, it has been proposed that a model that has this interaction at the *neural* level would more accurately reflect what occurs in the brain [27]. Specifically, one would need to deconvolve the seed region BOLD signal time course with the HRF to obtain its underlying neural activity time course. This deconvolved neural time course is then multiplied element-wise with the (unconvolved) experimental design or task variable. Finally, this product term is convolved with HRF to generate the interaction term that like other variables is at the hemodynamic level. The difference between the traditional and updated approaches can be illustrated in the following formulas:

$$\text{Interaction at the hemodynamic level : } x \cdot H(C)$$

$$\text{Interaction at the neural level : } H(H^{-1}(x) \cdot C)$$

where  $H^{-1}$  denotes the inverse of HRF convolution, i.e., deconvolution. Research has found that this deconvolution procedure has a large impact and is recommended when the task variable changes more rapidly than the hemodynamic response, i.e., in event-related designs [26, 27]. Moreover, taking the original, no-deconvolution approach can lead to spurious results if one also does not center the convolved psychological variable, whereas there is no such concern for the approach with deconvolution [28].

Third, in an attempt to examine inter-regional connections across the brain without arbitrary assumptions of their directionality, the correlational PPI (cPPI) adaptation of the PPI approach replaces the linear regression model with a partial correlation framework to estimate task-modulated changes in connections that are undirected [29]. Specifically, regression-based PPI approaches consider the seed and target brain regions as parts of a system with a particular directionality, such that findings of amygdala-hippocampal connectivity using an amygdala seed should be interpreted differently from findings of amygdala-hippocampal connectivity using a hippocampal seed [30]. In cPPI, the relaxation of any directionality assumption makes this method more consistent with the conceptualization of functional connectivity and has implications for downstream analyses such as the use of graph theoretical measures (see Section 4).

<sup>2</sup> Notably, since there must be a particular direction for model building (i.e., target activity regressed on seed activity), the PPI approach is also considered a method for *effective connectivity* because it explicitly examines the influence of the seed region on the target [5, 22], though many prefer to describe results from PPI analyses simply as *functional connectivity*.

The abovementioned variations of PPI analyses have been used widely to probe task-dependent functional connectivity in different experimental conditions. A meta-analysis of nearly 300 sPPI and gPPI studies found that their results show specificity to the combination of seed region and task [31]. For example, Faul et al. performed sPPI analyses seeded in the hippocampus to investigate functional connectivity differences between autobiographical memory recall and different mental manipulations (e.g., shifting visual perspective, simulating an alternative outcome) of autobiographical memory [32]. Gold et al. applied gPPI to probe how amygdala functional connectivity with other regions changes within an individual when they are attending to three specific aspects of emotional stimuli; individual functional connectivity profiles were also compared across different anxiety and age groups [33]. To study the effects of transcranial magnetic stimulation on whole-brain functional connectivity patterns related to episodic memory encoding, Davis et al. implemented cPPI to compute the difference in functional connectivity between subsequently remembered and subsequently forgotten stimuli for all pairs of brain regions [34]. Notably, the authors then analyzed the whole-brain connectivity matrices using techniques from graph theory. We elaborate on this approach later in Section 4. With its methodological robustness, relatively easy implementation, and straightforward interpretation, PPI remains one of the most frequently used families of methods for task-based fMRI functional connectivity to date.

## 2.2. Beta series correlation

An alternative analytical approach to assess task-related functional connectivity is Beta Series Correlation or BSC [6]. As mentioned previously, it is possible to deconvolve a BOLD signal time course to recover its underlying neural activity time course, which is arguably more specific and informative of cognitive operations than the BOLD signal time course and is an essential procedure for functional connectivity computation in event-related designs. Therefore, BSC aims to directly quantify the relationship between different brain regions' neural activity as functional connectivity.

Specifically, BSC first performs deconvolution via general linear models (GLMs), yielding regression coefficients or  $\beta$ s that indicate a given brain region's neural activity at the level of individual experimental trials or events (e.g., presentation of an image). Of note, the obtained single-trial  $\beta$  estimates are also the basis for a range of multivariate pattern analyses (see Sections 3.1 and 3.2). The utility of the BSC approach has resulted in a more thorough consideration of the scenarios in which this modeling approach is appropriate, and how it might be optimized. In the original proposal of BSC, the deconvolution procedure is completed through a single GLM that contains each of  $N$  experimental trials as a single-trial regressor-of-interest, as well as nuisance covariates such as the translational and rotational head motion estimates [6,35]. This modeling approach is referred to as *least squares - all* (LSA; see Fig. 3A) since one model generates  $\beta$  estimates for all trials. However, LSA was later shown to work well only for event-related designs that contain relatively long inter-trial intervals [6,36,37]. An alternative modeling approach referred to as *least squares - separate* (LSS; see Fig. 3B) overcomes the limitation by constructing  $N$  separate GLMs in parallel, with each model estimating one  $\beta$  estimate for a given trial-of-interest while all other trials are accounted for in a single regressor [37].

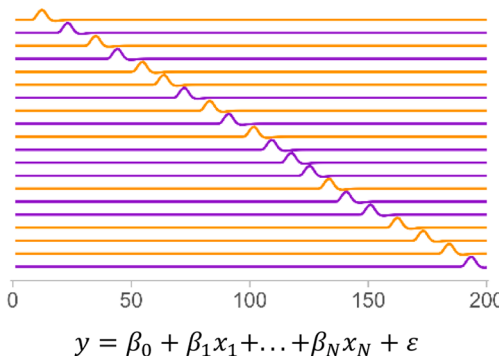
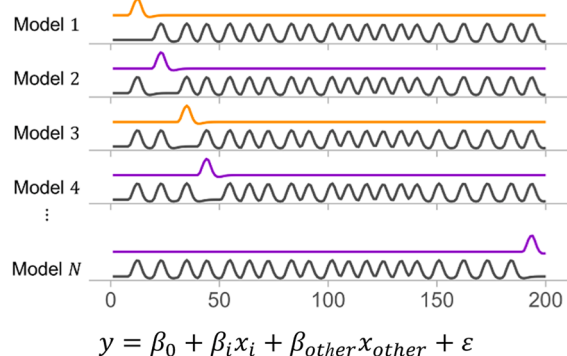
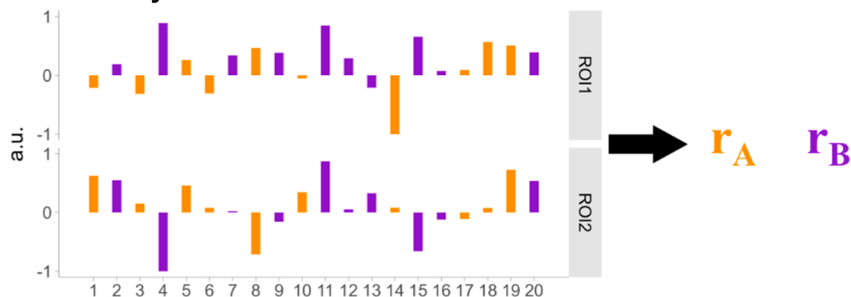
Regardless of the modeling choice for deconvolution, one obtains a series of  $\beta$  estimates, or a *beta series*, that indicates neural activity in all experimental trials. Then, the beta series are split by task conditions, and condition-wise beta series are correlated to compute functional connectivity (see Fig. 3C). Once connectivity estimates are obtained from all conditions and all participants, one typically proceeds to test group-level hypotheses using tests like *t*-test or ANOVA, or more complex graph theoretical approaches (see Section 4). For instance, Cooper et al. studied functional connectivity associated with encoding and retrieval processes of memory by computing beta series reflecting experimental trials in each task block and correlating them to construct process-specific functional connectivity networks; these networks were then compared between individuals with autism spectrum disorder and healthy controls [38]. Similarly, Deng et al. studied functional connectivity when participants were retrieving scene images. Based on individuals' subjective ratings of memory retrieval quality, the authors performed a within-participant split of experimental trials into high- and low-memory and constructed separate functional connectivity networks for each condition, which they further analyzed using a series of graph theoretical measures [39].

One major reason for the BSC method's growing popularity is its sensitivity to task-modulated changes in functional connectivity patterns relative to sPPI, especially for fast event-related fMRI designs, potentially owing to the deconvolution of hemodynamic responses at the single-trial level [24,26]. Another major difference between BSC and regression-based PPI approaches is the directionality of estimated connections, though cPPI is comparable to BSC since both would yield a symmetric connectivity matrix. Finally, the BSC method makes use of single-trial  $\beta$  estimates that track the neural activity associated with a specific event in the experiment, which are also often an indispensable part of several multi-voxel pattern analyses. We elaborate on the methodology in Section 3.

## 2.3. Multivariate techniques

The third analytical framework is a family of multivariate statistical methods that simultaneously assess the variances and covariance in many variables, such as the BOLD signal time courses of all voxels from an fMRI scan. There are various such multivariate techniques, including spectral clustering [40], principal components analysis (PCA; [41]), and independent components analysis (ICA; [42]). For example, ICA seeks to uncover statistically independent sources of variance from observed data.<sup>3</sup> All of these techniques

<sup>3</sup> Though ICA is more widely applied to resting-state fMRI data, some have incorporated it in task-based fMRI data analysis by fitting GLMs of experimental manipulations to time courses of independent components in order to assess the task-specificity of the components or networks [43, 44].

**A. Least squares all (LSA)****B. Least squares separate (LSS)****C. Single-trial betas by condition**

**Fig. 3. Beta series correlation (BSC).** **A**) The least squares - all (LSA) modeling approach constructs one general linear model (GLM) that contains  $N$  regressors, each of which models a single trial, and simultaneously estimates  $N$  regression coefficients ( $\beta_1, \dots, \beta_N$ ). Task conditions are color-coded (orange vs. purple). **B**) The least squares - separate (LSS) modeling approach constructs  $N$  GLMs in parallel. Each model contains one regressor for a single trial  $i$  of interest (color-coded by condition), as well as a regressor for all other trials across conditions (gray). Regression coefficients  $\beta_1, \dots, \beta_N$  are collected across models. Of note, for both LSA and LSS approaches, nuisance covariates such as motion parameters are commonly included in practice but omitted in the figure for simplicity. **C**) Regression coefficients or  $\beta$  values are split by task conditions to form *beta series*, which are then correlated between regions of interest (ROIs) to generate condition-specific functional connectivity.

enable data-driven grouping of voxels demonstrating similar spatiotemporal properties, and the identified groups can be used for connectivity analysis, instead of a priori modeling assumptions as in the PPI and BSC examples above.

The most commonly used multivariate technique for assessing task-related functional connectivity probably is *partial least squares* (PLS). Broadly, PLS has been used to examine whole-brain fMRI activity in relation to many kinds of variables, such as experimental conditions (design PLS), participant performance (behavior PLS), brain activity in a pre-selected region (seed PLS), or a combination of several factors (multiblock PLS) [45–48]. Specifically, seed PLS identifies brain regions whose activity series are associated with that of the seed region either commonly or distinctively across task conditions. The first step of seed PLS is generating correlation (or covariance) matrices for the seed brain regions, separately for each task condition, such that row  $j$  of the matrix reflects the whole-brain correlation pattern of seed  $j$  and the columns represent all targets. All these condition-wise correlation matrices are sorted in the same way for seed regions 1 to  $j$  and target regions 1 to  $k$ . Then, condition-wise correlation matrices are stacked vertically to form a correlation structure  $R$  (see Fig. 4B). Next, this correlation structure is factorized using singular value decomposition and converted to lower-dimensional latent variables (LVs) that summarize the commonalities and differences in the seed-brain correlations.<sup>4</sup>

Critically, even though seed PLS conceptualizes connectivity as correlation just like cPPI and BSC, the original seed PLS implementation computes the fundamental condition-wise correlation matrices at a different *level*. As mentioned above, PPI and BSC approaches compute functional connectivity for individual participants as the regression or correlation coefficient of time point- or trial-level activity, yielding *within-participant* functional connectivity. In contrast, seed PLS constructs the correlation matrices by correlating participant-level estimates of regional activity (e.g., percent signal change), yielding atemporal *across-participant* connectivity. A positive across-participant correlation coefficient indicates that participants with high activity in the seed region (relative to the sample mean) also tend to have high activity in the target region. For example, Spreng and Grady [50] employed seed PLS to analyze fMRI data of three self-referential tasks (cued autobiographical remembering, prospection, and theory-of-mind reasoning), finding an LV comprised of multiple default mode network regions whose participant-level activity was consistently correlated with that of a

<sup>4</sup> For a more detailed description on the computation and interpretation of latent variables, as well as significance testing for PLS, readers are referred to past review articles [45,49].

**A**

		Trial-level activity	Mean
Participant 1	Condition A	Seed	0.20
		Target 1	0.24
		Target 2	0.27
	Condition B	Seed	0.15
		Target 1	0.17
		Target 2	0.29
...		...	...
Participant 20	Condition A	Seed	0.09
		Target 1	0.14
		Target 2	0.16
	Condition B	Seed	0.14
		Target 1	0.08
		Target 2	0.16

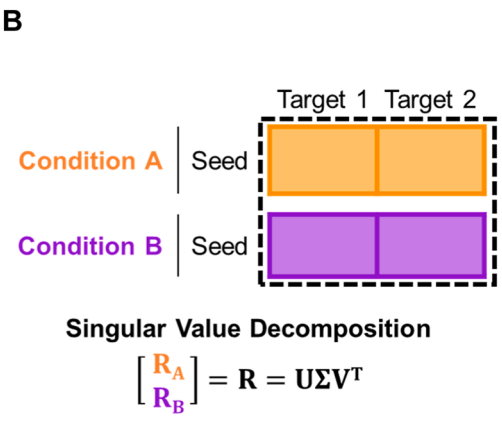


**Fig. 4.** Seed partial least squares (seed PLS) analysis. **A.** Synthetic trial-level activity series extracted from one seed and two target regions, organized by participant and task condition. Participant-and-condition-level activity can be estimated as the mean of relevant trial-level activities. **B.** Condition-wise cross-correlations for all seeds and targets are computed either *across-participant* (using participant-level activity) or *within-participant* (using trial-level activity). Correlation matrices are stacked vertically to form a correlation structure  $\mathbf{R}$ , which is factorized by singular value decomposition to extract latent variables.

medial prefrontal cortex seed region across all three tasks. Similarly, De Brigard et al. [51] conducted a seed PLS analysis to assess how the across-participant connectivity pattern of the right hippocampus differed across four different conditions of episodic counterfactual thinking.

Prior work has shown that across-participant and within-participant correlations are mathematically nonequivalent and often numerically incongruent [52], due to a statistical phenomenon called Simpson's Paradox [53]. However, seed PLS can be easily modified to investigate within-participant connectivity. For instance, one could first compute the correlation structure separately for each participant and then compute a group-average correlation structure  $R = \frac{1}{N} \sum_{k=1}^N R_k$  which is further analyzed with singular value decomposition [54]. Alternatively, one could directly examine the within-participant correlation structure using singular value decomposition and obtain LVs for each participant [52,55].

It is also worth noting that a key difference between PLS and other multivariate techniques for dimensionality reduction such as PCA and ICA is that PLS is a supervised method. PLS seeks a latent structure that maximizes the covariance between the data and an explicit target [56,57]. In the context of using seed PLS to analyze functional connectivity, the explicit target for covariance maximization is the fMRI activity time course of a pre-selected seed region in different conditions. The selection of the seed region is typically based on prior research or theories that suggest the critical involvement of this region for the cognitive function of interest. On the other hand, unsupervised methods such as PCA make no such pre-selection or assumption on the relevance of features (i.e., brain regions), and the extracted components are not biased by external criteria and more intrinsic to the studied system. Therefore, PCA can be applied to perform data-driven dimensionality reduction first, and then the extracted components can be used as regressors in a supervised model with other experimental or behavioral variables of interests (e.g., principal component regression) [58–60] to test explicit hypotheses regarding task-related functional connectivity.

### 3. Informational and representational connectivity

Given the millimeter-level spatial resolution of fMRI scans, a single ROI (e.g., left angular gyrus) may cover several hundred voxels, and each voxel has its own BOLD signal time course. In most functional connectivity frameworks (e.g., PPI, BSC), these voxel-wise BOLD signal time courses or their derivative neural activity series are averaged across voxels within the ROI to form one series that reflects regional fluctuations in activity, and functional connectivity is conceptualized as the inter-regional covariation of these series of *univariate* activity. Notably, although certain functional connectivity techniques like seed PLS do make use of *multivariate* statistical methods, those methods are implemented to decompose correlation structures whose constituent entries of correlation coefficients are still computed based on univariate activity series.

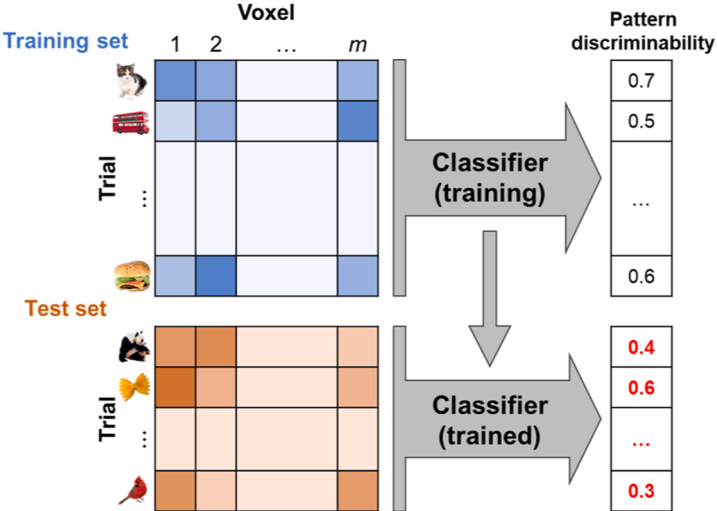
Following the concept of neural population coding [61] and methodological advancements in the past two decades, a paradigm shift in cognitive neuroscience has led to more investigations of the *spatially distributed multi-voxel pattern* of brain activity, which has

improved sensitivity to many cognitive processes relative to the across-voxel averaged univariate activity [62]. Relatedly, studies on the interaction between ROIs have built upon these new multi-voxel pattern analysis (MVPA) techniques to examine the inter-regional communication of information. In this Section, we review two major classes of MVPA-based connectivity analyses: informational connectivity and representational connectivity.

### 3.1. Informational connectivity

Informational connectivity refers to a generic class of analyses that quantify the inter-regional covariation in multi-voxel activity pattern discriminability [63]. A common approach to deriving an ROI's discriminability of discrete experimental conditions or stimulus types is decoding analysis [64], which typically involves four main steps. First, one decides which voxels are to be included, based on prior knowledge of functional localization or data-driven selection methods. Second, one re-organizes the selected voxels'

## A. Decoding analysis



## B. Representational similarity analysis

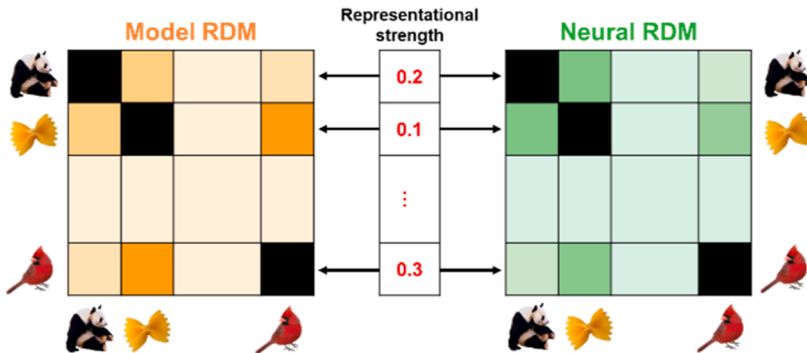


**Fig. 5.** A) Pattern discriminability series from decoding analysis. The multi-voxel activity patterns are organized by voxel and trial. The training set is used to train the classifier and will determine its decision criterion. The trained classifier is applied to the test set trials and generates a pattern discriminability series (red) indicating the magnitude of classifier evidence (e.g., probability) of individual trials belonging to the correct class. B) Representational strength series from representational similarity analysis. Representational dissimilarity matrices (RDMs) indicate the dissimilarity structure of the stimuli based on some hypothesis or model (model RDM) and their multi-voxel activity pattern (neural RDM). A row-wise correlation of these RDMs generates a representational strength series (red) which reflects the second-order correspondence between stimulus property and brain activity. The pattern discriminability series or representational strength series from distinct brain regions are correlated to compute informational connectivity or (model-based) representational connectivity, respectively.

BOLD or neural activity series as *patterns* such that the spatial distribution of those voxels is preserved across time points, with each time point having its own multi-voxel activity pattern. Third, one labels the activity pattern at each time point according to some discrete variable of interest, such as stimulus category (e.g., face vs. house) or behavior (e.g., correct vs. incorrect). Fourth, one chooses a *classifier*—a function that receives multi-voxel activity patterns as input and returns its best guess on each pattern’s label, i.e., decoding the experiences of participants in the experiment (see Fig. 5A). Of note, while the seminal work on decoding analysis used a relatively straightforward decision criterion based on correlation distance [65], later studies have made use of more sophisticated machine learning algorithms such as support vector machine and random forest to achieve better classification performance [62,66, 67].<sup>5</sup> Importantly, many have found decoding analysis to be more sensitive than traditional mass-univariate analysis, such as in detecting the respective roles of the medial prefrontal cortex in affective processing [72] and the ventral anterior temporal lobe in homonym comprehension [73].

Given a classifier’s output decision metric on each multi-voxel activity pattern, one could gather a trial-level series of pattern discriminability values that is analogous to the beta series in the BSC method. For any given ROI, these pattern discriminability values can fluctuate across trials in an experiment due to factors such as the typicality of the stimulus (e.g., “robin” is a more typical exemplar of “bird” than “ostrich”) and attentional lapses, as well as due to the influence of upstream regions in information processing. Then, just like how the BSC method computes functional connectivity as the correlation of beta series, the informational connectivity method computes the correlation coefficient of two ROI’s pattern discriminability series and quantifies the extent to which both regions’ multi-voxel activity patterns discriminate different stimulus identities [7,63]. High informational connectivity between two ROIs indicates that they tend to be synchronously (in)capable of discriminating stimulus identity, presumably due to their communication or exchange of task-relevant information.

The improved sensitivity of decoding analysis relative to univariate analysis is found to be preserved for informational connectivity relative to functional connectivity. In the pioneering fMRI study of informational connectivity where participants perceived images of man-made objects, informational connectivity delineated networks linking many canonical brain regions implicated in object processing (e.g., left fusiform gyrus, supramarginal gyrus) while functional connectivity measures failed to do so [63]. Similarly, in the visual processing domain, Ng et al. [74] computed multi-voxel pattern discriminability in different visual cortex layers for random dot stereograms and found that viewing binocular stereograms that supported a unified 3D perceptual experience was associated with enhanced feedforward informational connectivity relative to viewing those that did not, suggesting a bottom-up propagation of 3D structure information. Informational connectivity has also been applied to study semantic cognition. Soto et al. [75] found that deep processing of living and non-living words (i.e., imagining features related to a tiger like its shape, color, and context) rather than shallow processing (i.e., focusing on the phonology of “TIGER”) enhanced the semantic-category-based informational connectivity across regions commonly implicated in semantic cognition (e.g., left orbitofrontal cortex, anterior temporal lobe), while no significant difference in functional connectivity was observed.

Despite its improved sensitivity, the informational connectivity method inevitably suffers from the very limitations that are inherent to any decoding analysis (for a philosophical discussion on the issues, see [70]). For instance, simpler classifiers may be more interpretable but less accurate, while more sophisticated and powerful classifiers require a larger number of observations per class for training (e.g., [75] presented each of the 36 unique stimuli eight times). Given limited scanning time in many fMRI studies, repetitions of class labels necessitated by supervised learning inevitably constrain the variability of stimuli and thus impact the generalizability of results. Alternatively, one could use different exemplars from the same category, such as “cardinal”, “ostrich”, and “penguin” from the category “birds”. While this approach improves generalizability by reducing the likelihood of accidentally picking only idiosyncratic exemplars, the within- and between-category variability becomes less controllable (e.g., “birds” might be a more/less homogeneous category than “vehicles”), and concerns may arise with regards to whether these predefined categories are meaningful partitions of real-world entities—although this limitation may be addressed to some extent by representational similarity analysis.

### 3.2. Representational connectivity

Representational connectivity refers to a broad category of analyses that quantify the covariation in some representational properties of involved brain regions. In cognitive neuroscience, the term *representation*<sup>6</sup> refers to the neural response (e.g., a multi-voxel activity pattern) that is elicited by and stands in for some behaviorally relevant entity or concept, such as a stimulus image or an autobiographical memory [82,83]. For instance, when a participant scrutinizes a cat image, neural representations of the experience are sustained in the brain as a point in a high-dimensional representational space. Critically, a key signature of how a neural population or brain region represents our experiences is its *representational geometry*—i.e., the relative distances of its responses to different stimuli, which is often formalized as a representational dissimilarity matrix (RDM) that quantifies all pairwise dissimilarities using correlation distance or other measures [84,85]. RDMs are a centerpiece of representational similarity analysis and representational connectivity.

Because RDMs characterize representational geometries as matrices of the same size ( $m$ -by- $m$ , where  $m$  is the number of conditions

<sup>5</sup> There have been extensive discussions on the theoretical concerns or criticisms regarding different decoding methods [68,69,70,71], though this topic is beyond the scope of the current paper.

<sup>6</sup> A recent study surveyed the concept of *neural representation* according to philosophers, psychologists, and neuroscientists, finding general uncertainty amongst researchers about what counts as representation ([76]; cf. [77]). While this topic is beyond the scope of this review, interested readers are referred to other focused discussions (e.g., [78,79,80,81]).

or time points), one could conveniently quantify the similarity of two representational geometries by computing the correlation of their vectorized lower (or upper) triangular RDMS [86]. This measure is referred to as *model-free* representational connectivity since it requires no explicit hypothesis or model of the ROIs' representational geometries [87]. Previous work has found that representational connectivity reveals unique brain network structures that cannot be fully explained by univariate activation-based functional connectivity or other methods [88]. For instance, one study found a significant difference in representational connectivity but not functional connectivity among effort- and reward-related brain regions (i.e., anterior cingulate gyrus and anterior insula) for self- vs. other-benefiting behaviors [89], demonstrating the improved sensitivity of representational connectivity to the informational content of inter-regional communications. However, a limitation of model-free representational connectivity is the ambiguity in the exact type of information that is communicated between brain regions.

*Model-based* representational connectivity, on the contrary, characterizes the extent to which two brain regions represent similar information with respect to a hypothetical reference representational geometry. This reference can be based on formal theories [90, 91], behavioral response [92,93], or computational models [94,95], and it takes the form of a model RDM. The model RDM is compared to brain RDMS to obtain correspondence measures (i.e., representational strength) of hypothesized and observed representational geometries, as a key procedure in typical representational similarity analyses [85]. In one model-based representational connectivity approach, the representational strength measures are computed separately for different ROIs in all participants, and two ROIs are considered representationally connected if 1) the representational strength is significantly positive across participants in both ROIs and 2) their representational strengths are not significantly different [87].

Another approach to model-based representational connectivity makes use of condition- or trial-level estimates of representational strength. Specifically, instead of obtaining a single summary statistic for two representational geometries that span across all conditions and time points, one would perform a row-wise correlation between the model and brain RDMS [96–98] (see Fig. 5B). Subsequently, model-based representational connectivity can be calculated as the correlation of two ROIs' representational strength series, analogously to the computation of informational connectivity. No extant fMRI study to our knowledge has used this formulation of model-based representational connectivity to examine brain-wide communication of representations, though some have taken a multimodal approach to assessing inter-regional interactions.

### 3.3. A multimodal approach

As discussed above, both informational connectivity and model-based representational connectivity can be computed as the correlation of trial-level estimates of representational information, analogous to functional connectivity being computed as the correlation of trial-level betas. Notably, all those methods assess the statistical dependency based on the same neural measure of all involved brain regions (e.g., univariate activation, representational strength). However, these neural populations likely support distinct cognitive processes or have nonidentical mechanisms, to which different neural measures could be the most sensitive. As such, inter-regional connectivity or interaction may be best studied by not necessarily using the same neural measure for all regions but rather using what is most theoretically or empirically justified for each. For instance, studying the memory of emotional scenes, Ritchey et al. correlated trial-level estimates of *univariate activation* in the amygdala and *representational strength* in the cortex and found significantly stronger amygdala-cortical *connectivity* for remembered emotional scenes than for forgotten ones [99]. More recently, Huang et al. studied how participants' memory of concrete things could be supported by diverse hippocampal-cortical interactions during encoding. In particular, the interaction between hippocampal univariate activation and representational strength of semantic information in a semantic cognition region (left inferior frontal gyrus) predicted conceptual memory of the items, whereas the interaction between hippocampal univariate activation and representational strength of visual properties in a visual processing region (ventro-medial occipital cortex) predicted perceptual memory of the image exemplars [97]. These findings demonstrate the value of considering a multimodal approach in assessing inter-regional interaction or connectivity.

## 4. Building upon bivariate correlations—network analyses

Be it univariate-activation-based functional connectivity (e.g., PPI and BSC) or multivariate-activity-pattern-based informational or representational connectivity methods, the immediate output speaks to the covariation between only two brain regions, i.e., bivariate connections. Such spatial specificity may be appropriate and desirable when probing relatively simple interactions, yet complex cognition often involves the contribution of numerous brain areas that collectively form a functional *network* or *connectome*. A functional network or connectome is typically operationalized by a connectivity matrix that is often derived from iteratively computing all pairwise connections using previously reviewed methods. While such an approach usually assumes independent bivariate relationships, techniques for adjustment (e.g., partial correlation) can also be employed. Following network construction, a diverse set of methodologies is available to researchers who wish to examine the connectivity matrix as a whole and extract characteristics of the network that are not detectable at the local, pairwise level—global network properties that are uniquely informative of cognition.

### 4.1. Graph theoretical measures

Graph theory is a branch of mathematics that concerns the analysis of graphs, which are composed of a collection of *nodes* (or vertices) connected by *edges*, abstractly capturing the relationship between different entities. Mathematically, a graph can be defined by its adjacency or connection matrix, with its rows and columns representing individual nodes and its entry  $(i, j)$  recording the

presence or strength of the connection between node  $i$  and node  $j$  (see Fig. 1E). The brain can also be abstracted as a graph, with individual brain regions abstracted as nodes and their edges defined as structural connectivity measured by diffusion tensor imaging (DTI) or as functional connectivity estimated from fMRI data [100,101]. In most applications of graph theory to neuroimaging data, graphs are *undirected* (i.e., the connectivity from node  $i$  to node  $j$  is the same as that from node  $j$  to node  $i$ ). Graphs of the brain are also commonly *weighted*, where the edges are quantified by the strengths of connections (e.g., correlation coefficients) between a pair of regions, though connections could be binarized with some arbitrary threshold (e.g., edge = 1 if  $r > 0.2$ ) to deliver an *unweighted* graph.

A most attractive feature of treating the brain as a graph is that this approach offers a range of different graph theoretical measures that characterize different *nodal* properties of a single brain region in the context of the whole graph. For instance, a variety of indices quantify the extent to which a node is integrated with the graph, i.e., its centrality. For a given node, its nodal degree centrality is the number or sum of its connections. Slightly more complex centrality measures adjust for the fact that not all neighbors to which one node connects are equally important in the graph. For a given node, its connections to high-degree nodes make more contribution to communications throughout the network than connections to low-degree nodes, and therefore both Eigencentrality and PageRank centrality assign a high value to nodes who are well connected to other well-connected nodes [102]. Leverage centrality further considers the disparity in connectivity between a node and its immediate neighbors, assigning a high value to nodes that are better connected than their neighbors and are thus more influential in the vicinity [103].

Another set of indices concerns different *global* properties of graphs. Regarding how fast information may traverse though the network, the global efficiency index is computed as the average of the inverse of shortest distances [104]. The clustering coefficient quantifies how well-integrated a graph is by assessing the extent to which a node's neighbors are connected to each other (i.e., forming a triangle). For an unweighted graph, the clustering coefficient is defined as the average ratio of actual connections between any two neighbors of a node to all possible connections, averaged across all nodes in the graph [105], and there have been several generalizations of the clustering coefficient for weighted graphs [106]. Notably, many real-world systems, including the brain, exhibit both high global efficiency and high clustering; this feature is described as the networks' small-worldness, which is quantified by comparing the efficiency and clustering measures of a given graph to those of an equivalent Erdős-Rényi random graph [105,107,108]. Moreover, given a pre-defined community membership assignment of nodes (e.g., different lobes and hemispheres of the brain), the modularity measure quantifies the difference between the within-community connections of the actual network and that of a random structure, thereby indicating the quality of the partition of nodes [109]. In general, comparisons of such measures of global network properties across conditions or groups have become increasingly common. For example, Geerligs et al. [110] found that while global efficiency remains relatively stable across age groups, older adults demonstrate decreased modularity, suggesting an age-related increase in either the homogeneity of task-related signaling or noise. Additionally, graph theoretical measures describing the segregation of whole brain networks are often used as a starting point for evaluating sub-networks. We discuss this approach next.

#### 4.2. Community detection

Besides examining the properties of a graph at the nodal and global levels, another set of methods aims to organize the nodes as clusters or communities, based on the similarity of connectivity profiles between different nodes or the density of connections within proposed communities [111]. For instance, the Louvain method [112] seeks a community structure of the network that maximizes the previously mentioned modularity measure, and partitions the nodes into *nonoverlapping* modules or communities. Community detection subsequently enables the computation and interpretation of a whole other set of graph theoretical measures such as within-module degree, integration (ratio of between- to within-module degree), and participation coefficient (a node's in-module connections compared to its global connections). Alternatively, one may also opt to use canonical partitions of the brain based on resting-state connectivity, such as the 7-network structure generated by Yeo et al. [113]. However, no clear consensus has been reached concerning the demarcation or even the nomenclature of these "canonical" networks [20,18], and one should also be aware of the divergence between resting-state and task-based networks [114,115]. Moreover, it is critical to theoretically justify or statistically verify that the estimated or chosen community structure fits universally well to data from different populations (e.g., younger and older adults) or in different task conditions before conducting statistical tests on their differences [39].

Not all brain regions or communities are born equal. Research has shown the existence of network hub regions—nodes that are heavily involved in the communication between different functional modules and crucial for inter-module crosstalk (e.g., the angular gyrus and precuneus) [116,117]. Therefore, a rigid, all-or-none partition of brain regions into nonoverlapping modules is likely an oversimplification of the brain network structure. There have been attempts to organize brain regions into *overlapping* communities [118,119] using a variety of algorithms [120–122]. In addition, some brain regions may dynamically shift their affiliation with other networks as participants engage in various cognitive tasks [123,124] or perform at different levels [39,125]. Such kinds of brain dynamics would be missed by traditional analyses but can be captured by modeling different types of regional connections or interactions as different layers of a multilayer network [126]. Alternatively, multilayer networks can also be used to analyze different modalities altogether, such as incorporating fMRI-based functional connectivity with DTI-based structural connectivity [127].

#### 5. Limitations and future directions of connectivity

Despite their wide application in cognitive neuroscience research, the functional, informational, and representational connectivity techniques reviewed so far nonetheless suffer from at least three limitations or pitfalls: physiological noise, assumptions of linearity and stationarity, and level of analysis. We briefly discuss each of them below.

### 5.1. Low temporal sampling rate of fMRI

fMRI is noisy. In exchange for whole-brain coverage at a high spatial resolution, fMRI scans typically have a repetition time (TR) of around 2 s. This temporal sampling rate of 0.5 Hz is lower than the frequency of many physiological events that can introduce major artifacts in the measured BOLD signal, such as cardiac pulsations and respirations [128], as well as participant head movement inside the scanner [129]. Importantly, these physiological noises give rise to spurious correlations of activity not only in resting-state functional connectivity but also in task-based functional connectivity computed with BOLD signal [130].

Lots of effort has been put forth into separating the contributions of neural and physiological activities to BOLD signal ([131–133]; see also [134,135]). Specifically for task-based fMRI, neural activity estimated from the deconvolution of BOLD signal seems to suffer much less from the above issues and therefore does not show an inflated false positive rate of functional connectivity [6,136]. It is less known, however, how much these physiological artifacts impact the estimates from multi-voxel activity patterns such as pattern discriminability and representational strength, as well as the derived connectivity measures. Finally, increasing the temporal sampling rate of fMRI could also alleviate this issue by allowing statistical models to more effectively capture the physiological effects [137]. With more temporally precise characterization of the sequence of neural activations, faster fMRI could also open the door to better causal inferences based on statistical frameworks such as dynamic functional connectivity, Granger causality, and dynamic causal modeling [138–140].

### 5.2. Assumptions of linearity and stationarity

A notable feature of most connectivity analyses is that they are computed as the coefficient of Pearson's correlation or linear regression, which quantifies the *linear* relationship between variables. However, two variables (e.g., activity in two brain regions)

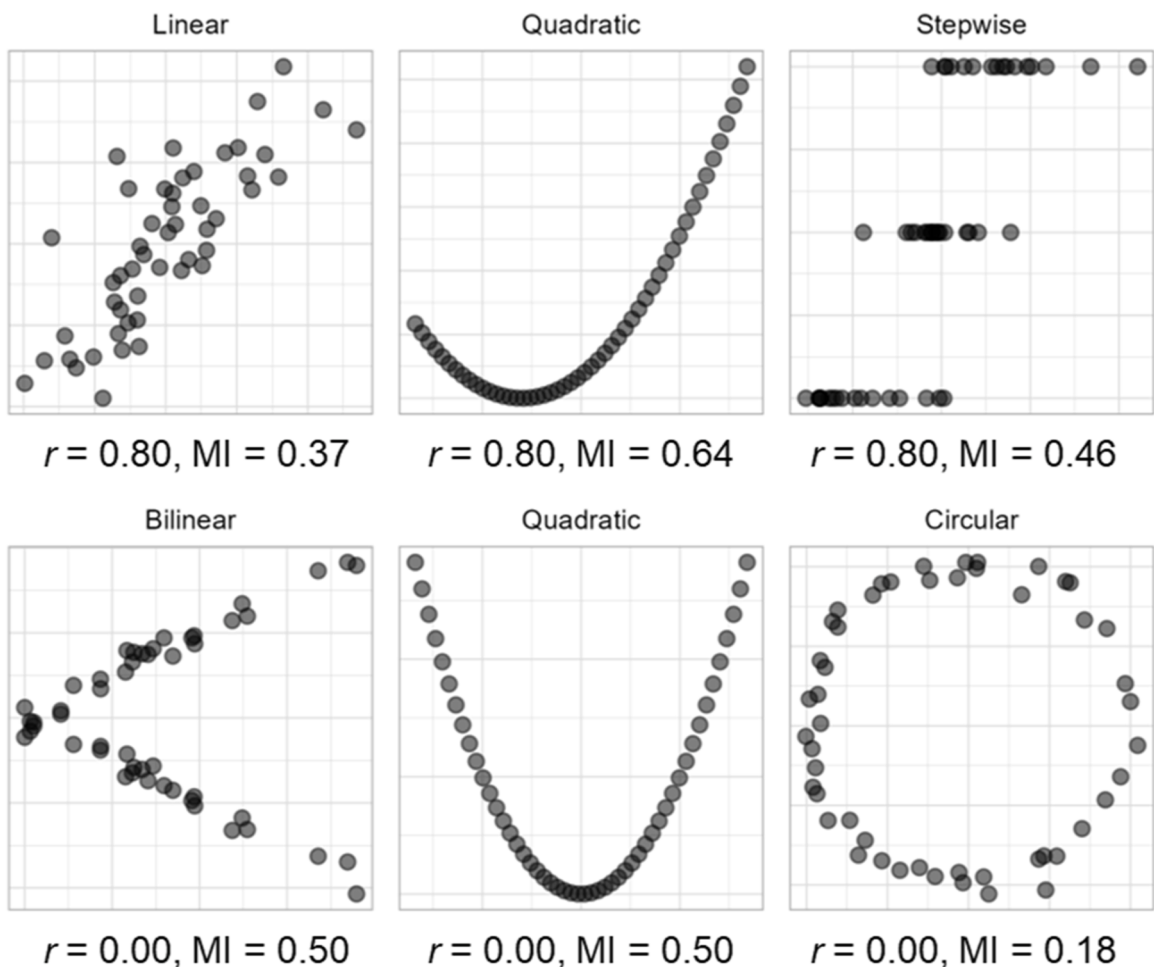


**Fig. 6.** Various statistical relationships between two random variables with 50 observations.  $r$ , Pearson correlation coefficient; MI, mutual information.

could also be statistically dependent on each other in various nonlinear ways where Pearson's correlation falls short in capturing them (see Fig. 6). Indeed, resting-state functional connectivity studies have found that certain inter-regional interactions are nonlinear [141–143], though some have argued that linear correlation is mostly sufficient in capturing most of the statistical dependence [144] and that observed nonlinear dependence may be spurious [145].

Regardless, one could employ a range of statistical tests to quantify nonlinear relationships. Both Spearman's  $\rho$  and Kendall's  $\tau$  measure the *ordinal* association of variables by ranking the observations instead of using their raw values (e.g., [146]), though the association is still assumed to be monotonic (i.e., a higher  $x$  is associated with a higher  $y$ ). In cases where higher-order relationships are reasonably expected, one could also first transform one of the variables according to the hypothesized order and then apply one of the linear or monotonic measures. Under the same rationale, a recently proposed method makes use of explicitly defined basis functions to capture the *functional coordinates* that indicate both the type and strength of diverse statistical associations [147]. Similarly, for regression, generalized additive models [148,149] use smooth functions to detect nonlinear relationships. Additionally, information theoretical measures such as mutual information (MI) [150,151] and variation of information [152], as well as distance correlation which applies to both univariate and multivariate data [153,154], are all able to capture the nonlinear statistical dependence between variables and can thus be used as alternative measures of connectivity.

Another common feature and limitation of fMRI connectivity analyses is that they assume stationarity in the relationships they assess, that is, the inter-regional interactions occur in some fixed timeframe. For instance, in PPI, the physiological time course of the dependent variable matches that of the independent variable TR-by-TR, assuming instantaneous effects from the seed to the target. Although one could introduce a fixed delay (e.g., 2 TRs) to one of the variables to estimate time-delayed effects, the modeled inter-regional interaction is still assumed to occur in a fixed or stationary timeframe. However, brain connectivity can occur dynamically at varying timeframes. While the present review is focused on functional connectivity that is time-locked to perceptual stimuli and externally cued tasks, models of resting-state connectivity have more freedom in characterizing spontaneous, dynamic changes in connectivity across the fMRI time course. Recurrence Quantification Analysis (RQA) is a useful tool for identifying the recurrence or alignment of matching sequences of two time series, and can be used to effectively generalize the cross-correlation function across time to capture the non-linear and non-stationary statistical dependence between two fMRI time courses [155,156]. To date, most work using RQA in fMRI has been focused on resting-state data [157–159]. Nevertheless, RQA may offer new insights to assessing brain network dynamics in task-related data as well.

### 5.3. Level of analysis

Most of the aforementioned methods estimate task-related connectivity at the level of individual participants. That is, regression or correlation coefficients quantifying the (linear) statistical relationship of brain regions are first computed within each participant, and then a subsequent test is used to investigate whether the connectivity estimates are significantly different from zero at the group-level (one-sample  $t$ -test), whether there are differences across experimental conditions (two-sample  $t$ -test or ANOVA), or how much these participant-level connectivity estimates associate with some behavioral variable (correlation or regression).

While this stepwise implementation is computationally convenient and widely adopted, some other methods estimate connectivity at a different level of analysis. As previously mentioned, the original seed PLS analysis computes the correlation of participant-level activity of brain regions, yielding a connectivity estimate across participants [45]. Notably, this *across-participant* connectivity is mathematically distinct from *within-participant* connectivity: a significant group-level effect may be absent (or even reversed) when examined in subgroups or individuals, a phenomenon known as Simpson's Paradox [53,52]. Yet another method called *inter-subject functional connectivity* (ISFC) computes the correlation of trial-level activity series across different participants [160]. While “*inter-subject*” appears interchangeable with “*across-subject*” or “*across-participant*”, ISFC is in fact more mathematically comparable to *intra-* or *within-participant* connectivity, while being able to eliminate biases from intrinsic connectivity within each participant [161, 162]. Ultimately, it is of critical importance to attend to these methodological details and determine the analytical approach—including the level of analysis—that best aligns with the hypothesis.

## 6. Concluding remarks

The notion of “brain connectivity” has undoubtedly led to abundant research into how different brain regions cooperate or compete to support complex cognitive processes and inspired the development of many advanced statistical methods for analyzing neuro-imaging data from task-based fMRI and other neuroimaging techniques, such as informational and representational connectivity. Despite the abundance of findings, the interpretability and comparability of results are unfortunately adversely impacted by methodological ambiguity and inconsistency. With this article, we aim to introduce and compare major techniques for task-based fMRI connectivity analyses, thereby clarifying points of confusion while also suggesting potential areas for future improvement. We stress that “connectivity” should not be regarded as a technical reference to one fixed set of analytical procedures but rather a generic umbrella term that encompasses many related approaches with nuanced but critical methodological divergences. Future research may use simulated fMRI data to provide more insight into the comparability of various kinds of statistical procedures. Overall, we hereby encourage future researchers to explicate as much as possible their conceptualizations of “connectivity” and their analytical procedures to minimize ambiguity and allow for meaningful cross-study comparisons and meta-analyses.

## Declaration of competing interest

The authors declare that they have no known competing financial interests or personal relationships that could have appeared to influence the work reported in this paper.

## Acknowledgments

SH, RC and SWD are supported by NIA 1RF1AG066901 and R01AG075417. FDB is supported by NSF FAIN 2218556.

## References

- [1] McCaffrey JB. Evolving Concepts of Functional Localization. *Philos. Compass* 2023;18:e12914. <https://doi.org/10.1111/phc3.12914>.
- [2] Kanwisher N, McDermott J, Chun MM. The Fusiform Face Area: A Module in Human Extrastriate Cortex Specialized for Face Perception. *J Neurosci* 1997;17:4302–11. <https://doi.org/10.1523/JNEUROSCI.17-11-04302.1997>.
- [3] Epstein R, Kanwisher N. A cortical representation of the local visual environment. *Nature* 1998;392:598–601. <https://doi.org/10.1038/33402>.
- [4] Bassett DS, Sporns O. Network neuroscience. *Nat Neurosci* 2017;20:353–64. <https://doi.org/10.1038/nn.4502>.
- [5] Friston KJ. Functional and effective connectivity in neuroimaging: A synthesis. *Hum. Brain Mapp* 1994;2:56–78. <https://doi.org/10.1002/hbm.460020107>.
- [6] Rissman J, Gazzaley A, D'Esposito M. Measuring functional connectivity during distinct stages of a cognitive task. *Neuroimage* 2004;23:752–63. <https://doi.org/10.1016/j.neuroimage.2004.06.035>.
- [7] Anzellotti S, Coutanche MN. Beyond Functional Connectivity: Investigating Networks of Multivariate Representations. *Trends Cogn. Sci.* 2018;22:258–69. <https://doi.org/10.1016/j.tics.2017.12.002>.
- [8] Horwitz B. The elusive concept of brain connectivity. *Neuroimage* 2003;19:466–70. [https://doi.org/10.1016/S1053-8119\(03\)00112-5](https://doi.org/10.1016/S1053-8119(03)00112-5).
- [9] Reid AT, Headley DB, Mill RD, Sanchez-Romero R, Uddin LQ, Marinazzo D, Lurie DJ, Valdés-Sosa PA, Hanson SJ, Biswal BB, Calhoun V, Poldrack RA, Cole MW. Advancing functional connectivity research from association to causation. *Nat Neurosci* 2019;22:1751–60. <https://doi.org/10.1038/s41593-019-0510-4>.
- [10] Fingelkurts Andrew A, Fingelkurts Alexander A, Kähkönen S. Functional connectivity in the brain—Is it an elusive concept? *Neurosci Biobehav Rev* 2005;28:827–36. <https://doi.org/10.1016/j.neubiorev.2004.10.009>.
- [11] Schaefer A, Kong R, Gordon EM, Laumann TO, Zuo XN, Holmes AJ, Eickhoff SB, Yeo BTT. Local-Global Parcellation of the Human Cerebral Cortex from Intrinsic Functional Connectivity MRI. *Cereb. Cortex* 2018;28:3095–114. <https://doi.org/10.1093/cercor/bhw179>.
- [12] Abraham A, Pedregosa F, Eickenberg M, Gervais P, Mueller A, Kossaifi J, Gramfort A, Thirion B, Varoquaux G. Machine learning for neuroimaging with scikit-learn. *Front. Neuroinformatics* 2014;8.
- [13] Bogdan PC, Iordan AD, Shobrook J, Dolcos F. ConnSearch: A framework for functional connectivity analysis designed for interpretability and effectiveness at limited sample sizes. *Neuroimage* 2023;278:120274. <https://doi.org/10.1016/j.neuroimage.2023.120274>.
- [14] Hunter JD. Matplotlib: A 2D Graphics Environment. *Comput Sci Eng* 2007;9:90–5. <https://doi.org/10.1109/MCSE.2007.55>.
- [15] Margulies DS, Böttger J, Watanabe A, Gorgolewski KJ. Visualizing the human connectome. *NeuroImage, Mapping the Connectome* 2013;80:445–61. <https://doi.org/10.1016/j.neuroimage.2013.04.111>.
- [16] Biswal B, Yetkin FZ, Haughton VM, Hyde JS. Functional connectivity in the motor cortex of resting human brain using echo-planar MRI. *Magn Reson Med* 1995;34:537–41. <https://doi.org/10.1002/mrm.1910340409>.
- [17] Buckner RL, Krienen FM, Yeo BTT. Opportunities and limitations of intrinsic functional connectivity MRI. *Nat Neurosci* 2013;16:832–7. <https://doi.org/10.1038/nn.3423>.
- [18] Uddin LQ, Yeo BTT, Spreng RN. Towards a Universal Taxonomy of Macro-scale Functional Human Brain Networks. *Brain Topogr* 2019;32:926–42. <https://doi.org/10.1007/s10548-019-00744-6>.
- [19] Zhang J, Kucyi A, Raya J, Nielsen AN, Nomi JS, Damoiseaux JS, Greene DJ, Horovitz SG, Uddin LQ, Whitfield-Gabrieli S. What have we really learned from functional connectivity in clinical populations? *Neuroimage* 2021;242:118466. <https://doi.org/10.1016/j.neuroimage.2021.118466>.
- [20] Uddin LQ, Betzel RF, Cohen JR, Damoiseaux JS, De Brigard F, Eickhoff SB, Fornito A, Gratton C, Gordon EM, Laird AR, Larson-Prior L, McIntosh AR, Nickerson LD, Pessoa L, Pinho AL, Poldrack RA, Razi A, Sadaghiani S, Shine JM, Yendiki A, Yeo BTT, Spreng RN. Controversies and progress on standardization of large-scale brain network nomenclature. *Netw Neurosci* 2023;1–42. [https://doi.org/10.1162/netn\\_a\\_00323](https://doi.org/10.1162/netn_a_00323).
- [21] Friston KJ, Buechel C, Fink GR, Morris J, Rolls E, Dolan RJ. Psychophysiological and Modulatory Interactions in Neuroimaging. *Neuroimage* 1997;6:218–29. <https://doi.org/10.1006/nimg.1997.0291>.
- [22] Friston KJ. Functional and Effective Connectivity: A Review. *Brain Connect* 2011;1:13–36. <https://doi.org/10.1089/brain.2011.0008>.
- [23] McLaren DG, Ries ML, Xu G, Johnson SC. A generalized form of context-dependent psychophysiological interactions (gPPI): A comparison to standard approaches. *Neuroimage* 2012;61:1277–86. <https://doi.org/10.1016/j.neuroimage.2012.03.068>.
- [24] Cisler JM, Bush K, Steele JS. A comparison of statistical methods for detecting context-modulated functional connectivity in fMRI. *Neuroimage* 2014;84:1042–52. <https://doi.org/10.1016/j.neuroimage.2013.09.018>.
- [25] O'Reilly JX, Woolrich MW, Behrens TEJ, Smith SM, Johansen-Berg H. Tools of the trade: psychophysiological interactions and functional connectivity. *Soc Cogn Affect Neurosci* 2012;7:604–9. <https://doi.org/10.1093/scan/nss055>.
- [26] Di X, Zhang Z, Biswal BB. Understanding psychophysiological interaction and its relations to beta series correlation. *Brai Imaging Behav* 2020. <https://doi.org/10.1007/s11682-020-00304-8>.
- [27] Gitelman DR, Penny WD, Ashburner J, Friston KJ. Modeling regional and psychophysiological interactions in fMRI: the importance of hemodynamic deconvolution. *Neuroimage* 2003;19:200–7. [https://doi.org/10.1016/S1053-8119\(03\)00058-2](https://doi.org/10.1016/S1053-8119(03)00058-2).
- [28] Di X, Reynolds RC, Biswal BB. Imperfect (de)convolution may introduce spurious psychophysiological interactions and how to avoid it. *Hum Brain Mapp* 2017;38:1723–40. <https://doi.org/10.1002/hbm.23413>.
- [29] Fornito A, Harrison BJ, Zalesky A, Simons JS. Competitive and cooperative dynamics of large-scale brain functional networks supporting recollection. *Proc. Natl. Acad. Sci.* 2012;109:12788–93. <https://doi.org/10.1073/pnas.1204185109>.
- [30] Stephan KE. On the role of general system theory for functional neuroimaging. *J Anat* 2004;205:443–70. <https://doi.org/10.1111/j.0021-8782.2004.00359.x>.
- [31] Smith DV, Gseir M, Speer ME, Delgado MR. Toward a cumulative science of functional integration: A meta-analysis of psychophysiological interactions. *Hum Brain Mapp* 2016;37:2904–17. <https://doi.org/10.1002/hbm.23216>.
- [32] Paul L, St. Jacques PL, DeRosa JT, Parikh N, De Brigard F. Differential contribution of anterior and posterior midline regions during mental simulation of counterfactual and perspective shifts in autobiographical memories. *Neuroimage* 2020;215:116843. <https://doi.org/10.1016/j.neuroimage.2020.116843>.
- [33] Gold AL, Shechner T, Farber MJ, Spiro CN, Leibenluft E, Pine DS, Britton JC. Amygdala-Cortical Connectivity: Associations with Anxiety, Development, and Threat. *Depress. Anxiety* 2016;33:917–26. <https://doi.org/10.1002/da.22470>.
- [34] Davis SW, Luber B, Murphy DLK, Lisanby SH, Cabeza R. Frequency-specific neuromodulation of local and distant connectivity in aging and episodic memory function. *Hum Brain Mapp* 2017;38:5987–6004. <https://doi.org/10.1002/hbm.23803>.
- [35] Daselaar SM, Fleck MS, Cabeza R. Triple Dissociation in the Medial Temporal Lobes: Recollection, Familiarity, and Novelty. *J Neurophysiol* 2006;96:1902–11. <https://doi.org/10.1152/jn.01029.2005>.

- [36] Abdulrahman H, Henson RN. Effect of trial-to-trial variability on optimal event-related fMRI design: Implications for Beta-series correlation and multi-voxel pattern analysis. *Neuroimage* 2016;125:756–66. <https://doi.org/10.1016/j.neuroimage.2015.11.009>.
- [37] Mumford JA, Turner BO, Ashby FG, Poldrack RA. Deconvolving BOLD activation in event-related designs for multivoxel pattern classification analyses. *Neuroimage* 2012;59:2636–43. <https://doi.org/10.1016/j.neuroimage.2011.08.076>.
- [38] Cooper RA, Richter FR, Bays PM, Plaisted-Grant KC, Baron-Cohen S, Simons JS. Reduced Hippocampal Functional Connectivity During Episodic Memory Retrieval in Autism. *Cereb. Cortex* 2017;27:888–902. <https://doi.org/10.1093/cercor/bhw417>.
- [39] Deng L, Stanley ML, Monge ZA, Wing EA, Geib BR, Davis SW, Cabeza R. Age-Related Compensatory Reconfiguration of PFC Connections during Episodic Memory Retrieval. *Cereb. Cortex* 2021;31:717–30. <https://doi.org/10.1093/cercor/bhaa192>.
- [40] Craddock RC, James GA, Holtzheimer III PE, Hu XP, Mayberg HS. A whole brain fMRI atlas generated via spatially constrained spectral clustering. *Hum. Brain Mapp* 2012;33:1914–28. <https://doi.org/10.1002/hbm.21333>.
- [41] Liu J, Xu L, Caprihana A, Calhoun VD. Extracting principle components for discriminant analysis of fMRI images. In: 2008 IEEE International Conference on Acoustics, Speech and Signal Processing. Presented at the 2008 IEEE International Conference on Acoustics, Speech and Signal Processing; 2008. p. 449–52. <https://doi.org/10.1109/ICASSP.2008.4517643>.
- [42] McKeown MJ, Makeig S, Brown GG, Jung TP, Kindermann SS, Bell AJ, Sejnowski TJ. Analysis of fMRI data by blind separation into independent spatial components. *Hum. Brain Mapp* 1998;6:160–88. [https://doi.org/10.1002/\(SICI\)1097-0193\(1998\)6:3<160::AID-HBMS>3.0.CO;2-1](https://doi.org/10.1002/(SICI)1097-0193(1998)6:3<160::AID-HBMS>3.0.CO;2-1).
- [43] Campbell KL, Samu D, Davis SW, Geerlings L, Mustafa A, Tyler LK. Neuroscience for CCfor Aand. Robust Resilience of the Frontotemporal Syntax System to Aging. *J Neurosci* 2016;36:5214–27. <https://doi.org/10.1523/JNEUROSCI.4561-15.2016>.
- [44] Davis SW, Zhuang J, Wright P, Tyler LK. Age-related sensitivity to task-related modulation of language-processing networks. *Neuropsychologia* 2014;63:107–15. <https://doi.org/10.1016/j.neuropsychologia.2014.08.017>.
- [45] Krishnan A, Williams LJ, McIntosh AR, Abdi H. Partial Least Squares (PLS) methods for neuroimaging: A tutorial and review. *NeuroImage, Multivariate Decoding and Brain Reading* 2011;56:455–75. <https://doi.org/10.1016/j.neuroimage.2010.07.034>.
- [46] McIntosh AR, Bookstein FL, Haxby JV, Grady CL. Spatial Pattern Analysis of Functional Brain Images Using Partial Least Squares. *Neuroimage* 1996;3:143–57. <https://doi.org/10.1006/nimg.1996.0016>.
- [47] McIntosh AR, Lobaugh NJ, Cabeza R, Bookstein FL, Houle S. Convergence of neural systems processing stimulus associations and coordinating motor responses. *Cereb. Cortex* 1998;8:648–59. <https://doi.org/10.1093/cercor/8.7.648>.
- [48] McIntosh AR, Chau WK, Protzner AB. Spatiotemporal analysis of event-related fMRI data using partial least squares. *Neuroimage* 2004;23:764–75. <https://doi.org/10.1016/j.neuroimage.2004.05.018>.
- [49] Mwangi B, Tian TS, Soares JC. A Review of Feature Reduction Techniques in Neuroimaging. *Neuroinformatics* 2014;12:229–44. <https://doi.org/10.1007/s12021-013-9204-3>.
- [50] Spreng RN, Grady CL. Patterns of Brain Activity Supporting Autobiographical Memory, Prospection, and Theory of Mind, and Their Relationship to the Default Mode Network. *J Cogn Neurosci* 2010;22:1112–23. <https://doi.org/10.1162/jocn.2009.21282>.
- [51] De Brigard F, Nathan Spreng R, Mitchell JP, Schacter DL. Neural activity associated with self, other, and object-based counterfactual thinking. *Neuroimage* 2015;109:12–26. <https://doi.org/10.1016/j.neuroimage.2014.12.075>.
- [52] Roberts RP, Hach S, Tippett LJ, Addis DR. The Simpson's paradox and fMRI: Similarities and differences between functional connectivity measures derived from within-subject and across-subject correlations. *Neuroimage* 2016;135:1–15. <https://doi.org/10.1016/j.neuroimage.2016.04.028>.
- [53] Kievit R, Frankenhuus W, Waldorp L, Borsboom D. Simpson's paradox in psychological science: a practical guide. *Front Psychol* 2013;4.
- [54] Bellanca B, Liu ZX, Diamond NB, Grady CL, Moscovitch M. Similarities and differences in the default mode network across rest, retrieval, and future imagining. *Hum Brain Mapp* 2017;38:1155–71. <https://doi.org/10.1002/hbm.23445>.
- [55] Roberts RP, Wiebels K, Sumner RL, van Mulukom V, Grady CL, Schacter DL, Addis DR. An fMRI investigation of the relationship between future imagination and cognitive flexibility. *Neuropsychologia* 2017;95:156–72. <https://doi.org/10.1016/j.neuropsychologia.2016.11.019>.
- [56] Barshan E, Ghodsi A, Azimifard Z, Zolghadri Jahromi M. Supervised principal component analysis: Visualization, classification and regression on subspaces and submanifolds. *Pattern Recognit* 2011;44:1357–71. <https://doi.org/10.1016/j.patcog.2010.12.015>.
- [57] Moindjé IA, Dabo-Niang S, Preda C. Classification of multivariate functional data on different domains with Partial Least Squares approaches. *Stat Comput* 2023;34:5. <https://doi.org/10.1007/s11222-023-10324-1>.
- [58] Agarwal A, Shah D, Shen D, Song D. On Robustness of Principal Component Regression. *J Am Stat Assoc* 2021;116:1731–45. <https://doi.org/10.1080/01621459.2021.1928513>.
- [59] Shahhosseini Y, Miranda MF. Functional Connectivity Methods and Their Applications in fMRI Data. *Entropy* 2022;24:390. <https://doi.org/10.3390/e24030390>.
- [60] Zhong Y, Wang H, Lu G, Zhang Z, Jiao Q, Liu Y. Detecting Functional Connectivity in fMRI Using PCA and Regression Analysis. *Brain Topogr* 2009;22:134–44. <https://doi.org/10.1007/s10548-009-0095-4>.
- [61] Pouget A, Dayan P, Zemel R. Information processing with population codes. *Nat Rev Neurosci* 2000;1:125–32. <https://doi.org/10.1038/35039062>.
- [62] Weaverdyck ME, Lieberman MD, Parkinson C. Tools of the Trade Multivoxel pattern analysis in fMRI: a practical introduction for social and affective neuroscientists. *Soc Cogn Affect Neurosci* 2020;15:487–509. <https://doi.org/10.1093/scan/nsaa057>.
- [63] Coutanche MN, Thompson-Schill SL. Informational connectivity: identifying synchronized discriminability of multi-voxel patterns across the brain. *Front Hum Neurosci* 2013;7. <https://doi.org/10.3389/fnhum.2013.00015>.
- [64] Norman KA, Polyn SM, Detre GJ, Haxby JV. Beyond mind-reading: multi-voxel pattern analysis of fMRI data. *Trends Cogn. Sci.* 2006;10:424–30. <https://doi.org/10.1016/j.tics.2006.07.005>.
- [65] Haxby JV, Gobbini MI, Furey ML, Ishai A, Schouten JL, Pietrini P. Distributed and Overlapping Representations of Faces and Objects in Ventral Temporal Cortex. *Science* (1979) 2001;293:2425–30. <https://doi.org/10.1126/science.1063736>.
- [66] Kuntzelman KM, Williams JM, Lim PC, Samal A, Rao PK, Johnson MR. Deep-Learning-Based Multivariate Pattern Analysis (dMVPA): A Tutorial and a Toolbox. *Front Hum Neurosci* 2021:15.
- [67] Misaki M, Kim Y, Bandettini PA, Kriegeskorte N. Comparison of multivariate classifiers and response normalizations for pattern-information fMRI. *Neuroimage* 2010;53:103–18. <https://doi.org/10.1016/j.neuroimage.2010.05.051>.
- [68] Anderson M, Oates T. A critique of multi-voxel pattern analysis. *Proc. Annu. Meet. Cogn. Sci. Soc.* 2010;32.
- [69] Carlson T, Goddard E, Kaplan DM, Klein C, Ritchie JB. Ghosts in machine learning for cognitive neuroscience: Moving from data to theory. *NeuroImage, New advances in encoding and decoding of brain signals* 2018;180:88–100. <https://doi.org/10.1016/j.neuroimage.2017.08.019>.
- [70] Gessell B, Geib B, De Brigard F. Multivariate pattern analysis and the search for neural representations. *Synthese* 2021. <https://doi.org/10.1007/s11229-021-03358-3>.
- [71] Ritchie JB, Kaplan DM, Klein C. Decoding the Brain: Neural Representation and the Limits of Multivariate Pattern Analysis in Cognitive Neuroscience. *Br J Philos Sci* 2019;70:581–607. <https://doi.org/10.1093/bjps/axx023>.
- [72] Peelen MV, Atkinson AP, Vuilleumier P. Supramodal Representations of Perceived Emotions in the Human Brain. *J Neurosci* 2010;30:10127–34. <https://doi.org/10.1523/JNEUROSCI.2161-10.2010>.
- [73] Hoffman P, Tammi A. Barking up the right tree: Univariate and multivariate fMRI analyses of homonym comprehension. *Neuroimage* 2020;219:117050. <https://doi.org/10.1016/j.neuroimage.2020.117050>.
- [74] Ng AKT, Jia K, Goncalves NR, Zamboni E, Kemper VG, Goebel R, Welchman AE, Kourtzi Z. Ultra-High-Field Neuroimaging Reveals Fine-Scale Processing for 3D Perception. *J Neurosci* 2021;41:8362–74. <https://doi.org/10.1523/JNEUROSCI.0065-21.2021>.
- [75] Soto D, Sheikholeslami A, Mei N, Santana R. Decoding and encoding models reveal the role of mental simulation in the brain representation of meaning. *R. Soc. Open Sci.* 2020;7:192043. <https://doi.org/10.1098/rsos.192043>.
- [76] Favela LH, Machery E. Investigating the concept of representation in the neural and psychological sciences. *Front Psychol* 2023;14.

- [77] Richmond A. Commentary: Investigating the concept of representation in the neural and psychological sciences. *Front Psychol* 2023;14.
- [78] Baker B, Lansdell B, Kording KP. Three aspects of representation in neuroscience. *Trends Cogn. Sci.* 2022;26:942–58. <https://doi.org/10.1016/j.tics.2022.08.014>.
- [79] Cao R. Putting representations to use. *Synthese* 2022;200:151. <https://doi.org/10.1007/s11229-022-03522-3>.
- [80] Robins SK, De Brigard F, editors. *Interdisciplinary perspectives on locating representations in the brain*. *Synthese*; 2024.
- [81] Roskies AL. Representational similarity analysis in neuroimaging: proxy vehicles and provisional representations. *Synthese* 2021;199:5917–35. <https://doi.org/10.1007/s11229-021-03052-4>.
- [82] Edelman S, Grill-Spector K, Kushnir T, Malach R. Toward direct visualization of the internal shape representation space by fMRI. *Psychobiology* 1998;26:309–21. <https://doi.org/10.3758/BF03330618>.
- [83] Thomson E, Piccinini G. Neural Representations Observed. *Minds Mach.* 2018;28:191–235. <https://doi.org/10.1007/s11023-018-9459-4>.
- [84] Bobadilla-Suarez S, Ahlheim C, Mehrotra A, Panos A, Love BC. Measures of Neural Similarity. *Comput Brain Behav* 2020;3:369–83. <https://doi.org/10.1007/s42113-019-00068-5>.
- [85] Kriegeskorte N, Kievit RA. Representational geometry: integrating cognition, computation, and the brain. *Trends Cogn. Sci.* 2013;17:401–12. <https://doi.org/10.1016/j.tics.2013.06.007>.
- [86] Kriegeskorte N, Mur M, Bandettini P. Representational similarity analysis - connecting the branches of systems neuroscience. *Front Syst Neurosci* 2008;2.
- [87] Karimi-Rouzbehani H, Woolgar A, Henson R, Nili H. Caveats and Nuances of Model-Based and Model-Free Representational Connectivity Analysis. *Front Neurosci* 2022;16.
- [88] Pillet I, Op de Beech H, Lee Masson H. A Comparison of Functional Networks Derived From Representational Similarity, Functional Connectivity, and Univariate Analyses. *Front Neurosci* 2020;13.
- [89] Lockwood PL, Wittmann MK, Nili H, Matsumoto-Ryan M, Abdurahman A, Cutler J, Husain M, Apps MAJ. Distinct neural representations for prosocial and self-benefiting effort. *Curr Biol* 2022;32:4172–85. <https://doi.org/10.1016/j.cub.2022.08.010>. e7.
- [90] Cetron JS, Connolly AC, Diamond SG, May VV, Haxby JV, Kraemer DJM. Decoding individual differences in STEM learning from functional MRI data. *Nat Commun* 2019;10:1–10. <https://doi.org/10.1038/s41467-019-10053-y>.
- [91] Clarke A, Tyler LK. Object-Specific Semantic Coding in Human Perirhinal Cortex. *J Neurosci* 2014;34:4766–75. <https://doi.org/10.1523/JNEUROSCI.2828-13.2014>.
- [92] King ML, Groen IIA, Steel A, Kravitz DJ, Baker CI. Similarity judgments and cortical visual responses reflect different properties of object and scene categories in naturalistic images. *Neuroimage* 2019;197:368–82. <https://doi.org/10.1016/j.neuroimage.2019.04.079>.
- [93] Liuzzi AG, Bruffaerts R, Dupont P, Adamczuk K, Peeters R, De Deyne S, Storms G, Vandenberghe R. Left perirhinal cortex codes for similarity in meaning between written words: Comparison with auditory word input. *Neuropsychologia*, Special Issue: Semantic Cognition 2015;76:4–16. <https://doi.org/10.1016/j.neuropsychologia.2015.03.016>.
- [94] Cichy RM, Khosla A, Pantazis D, Torralba A, Oliva A. Comparison of deep neural networks to spatio-temporal cortical dynamics of human visual object recognition reveals hierarchical correspondence. *Sci Rep* 2016;6:27755. <https://doi.org/10.1038/srep27755>.
- [95] Deng L, Davis SW, Monge ZA, Wing EA, Geib BR, Raghunandan A, Cabeza R. Age-related dedifferentiation and hyperdifferentiation of perceptual and mnemonic representations. *Neurobiol Aging* 2021;106:55–67. <https://doi.org/10.1016/j.neurobiolaging.2021.05.021>.
- [96] Davis SW, Geib BR, Wing EA, Wang WC, Hovhannissyan M, Monge ZA, Cabeza R. Visual and Semantic Representations Predict Subsequent Memory in Perceptual and Conceptual Memory Tests. *Cereb. Cortex* 2021;31:974–92. <https://doi.org/10.1093/cercor/bhaa269>.
- [97] Huang S, Howard CM, Hovhannissyan M, Ritchey M, Cabeza R, Davis SW. Hippocampal functions modulate transfer-appropriate cortical representations supporting subsequent memory. *J Neurosci* 2023. <https://doi.org/10.1523/JNEUROSCI.1135-23.2023>.
- [98] Naspi L, Stensholt C, Karlsson AE, Monge ZA, Cabeza R. Effects of Aging on Successful Object Encoding: Enhanced Semantic Representations Compensate for Impaired Visual Representations. *J Neurosci* 2023;43:7337–50. <https://doi.org/10.1523/JNEUROSCI.2265-22.2023>.
- [99] Ritchey M, Wing EA, LaBar KS, Cabeza R. Neural Similarity Between Encoding and Retrieval is Related to Memory Via Hippocampal Interactions. *Cereb. Cortex* 2013;23:2818–28. <https://doi.org/10.1093/cercor/bhs258>.
- [100] Farahani FV, Karwowski W, Lighthall NR. Application of Graph Theory for Identifying Connectivity Patterns in Human Brain Networks: A Systematic Review. *Front Neurosci* 2019;13. <https://doi.org/10.3389/fnins.2019.00585>.
- [101] Rubinov M, Sporns O. Complex network measures of brain connectivity: Uses and interpretations. *NeuroImage, Computational Models of the Brain* 2010;52:1059–69. <https://doi.org/10.1016/j.neuroimage.2009.10.003>.
- [102] Zuo XN, Ehmke R, Mennes M, Imperati D, Castellanos FX, Sporns O, Milham MP. Network Centrality in the Human Functional Connectome. *Cereb. Cortex* 2012;22:1862–75. <https://doi.org/10.1093/cercor/bhr269>.
- [103] Joyce KE, Laurienti PJ, Burdette JH, Hayasaka S. A New Measure of Centrality for Brain Networks. *PLoS One* 2010;5:e12200. <https://doi.org/10.1371/journal.pone.0012200>.
- [104] Latora V, Marchiori M. Efficient Behavior of Small-World Networks. *Phys Rev Lett* 2001;87:198701. <https://doi.org/10.1103/PhysRevLett.87.198701>.
- [105] Watts DJ, Strogatz SH. Collective dynamics of ‘small-world’ networks. *Nature* 1998;393:440–2. <https://doi.org/10.1038/30918>.
- [106] Wang Y, Ghumare E, Vandenberghe R, Dupont P. Comparison of Different Generalizations of Clustering Coefficient and Local Efficiency for Weighted Undirected Graphs. *Neural Comput* 2017;29:313–31. [https://doi.org/10.1162/NECO\\_a\\_00914](https://doi.org/10.1162/NECO_a_00914).
- [107] Humphries MD, Gurney K. Network ‘Small-World-Ness’: A Quantitative Method for Determining Canonical Network Equivalence. *PLoS One* 2008;3:e0002051. <https://doi.org/10.1371/journal.pone.0002051>.
- [108] Muldoon SF, Bridgeford EW, Bassett DS. Small-World Propensity and Weighted Brain Networks. *Sci Rep* 2016;6:22057. <https://doi.org/10.1038/srep22057>.
- [109] Newman MEJ, Girvan M. Finding and evaluating community structure in networks. *Phys Rev E* 2004;69:026113. <https://doi.org/10.1103/PhysRevE.69.026113>.
- [110] Geerligs L, Renken RJ, Saliasi E, Maurits NM, Lorist MM. A Brain-Wide Study of Age-Related Changes in Functional Connectivity. *Cereb. Cortex* 2015;25:1987–99. <https://doi.org/10.1093/cercor/bhu012>.
- [111] Sporns O, Betzel RF. Modular Brain Networks. *Annu Rev Psychol* 2016;67:613–40. <https://doi.org/10.1146/annurev-psych-122414-033634>.
- [112] Blondel VD, Guillaume JL, Lambiotte R, Lefebvre E. Fast unfolding of communities in large networks. *J. Stat. Mech. Theory Exp.* 2008;P10008. <https://doi.org/10.1088/1742-5468/2008/10/P10008>. 2008.
- [113] Yeo BT, Krienen FM, Sepulcre J, Sabuncu MR, Lashkari D, Hollinshead M, Roffman JL, Smoller JW, Zöllei L, Polimeni JR, Fischl B, Liu H, Buckner RL. The organization of the human cerebral cortex estimated by intrinsic functional connectivity. *J Neurophysiol* 2011;106:1125–65. <https://doi.org/10.1152/jn.00338.2011>.
- [114] Di X, Goel S, Kim EH, Biswal BB. Task vs. rest—Different network configurations between the coactivation and the resting-state brain networks. *Front Hum Neurosci* 2013;7:56300. <https://doi.org/10.3389/fnhum.2013.00493>.
- [115] Elliott ML, Knott AR, Cooke M, Kim MJ, Melzer TR, Keenan R, Ireland D, Ramrakha S, Poultney R, Caspi A, Moffitt TE, Hariri AR. General functional connectivity: Shared features of resting-state and task fMRI drive reliable and heritable individual differences in functional brain networks. *NeuroImage* 2019;189:516–32. <https://doi.org/10.1016/j.neuroimage.2019.01.068>.
- [116] Power JD, Schlaggar BL, Lessov-Schlaggar CN, Petersen SE. Evidence for hubs in human functional brain networks. *Neuron* 2013;79. <https://doi.org/10.1016/j.neuron.2013.07.035>.
- [117] van den Heuvel MP, Sporns O. Network hubs in the human brain. *Trends Cogn. Sci., Special Issue: The Connectome* 2013;17:683–96. <https://doi.org/10.1016/j.tics.2013.09.012>.
- [118] Gu Y, Li L, Zhang Y, Ma J, Yang C, Xiao Y, Shu N, Can C, Lin Y, Dai Z. The overlapping modular organization of human brain functional networks across the adult lifespan. *Neuroimage* 2022;253:119125. <https://doi.org/10.1016/j.neuroimage.2022.119125>.

- [119] Najafi M, McMenamin BW, Simon JZ, Pessoa L. Overlapping communities reveal rich structure in large-scale brain networks during rest and task conditions. *NeuroImage* 2016;135:92–106. <https://doi.org/10.1016/j.neuroimage.2016.04.054>.
- [120] Bai X, Yang P, Shi X. An overlapping community detection algorithm based on density peaks. *Neurocomputing* 2017;226:7–15. <https://doi.org/10.1016/j.neucom.2016.11.019>.
- [121] Cao X, Wang X, Jin D, Cao Y, He D. Identifying overlapping communities as well as hubs and outliers via nonnegative matrix factorization. *Sci Rep* 2013;3:2993. <https://doi.org/10.1038/srep02993>.
- [122] Fang C, Lin ZZ. Overlapping communities detection based on cluster-ability optimization. *Neurocomputing* 2022;494:336–45. <https://doi.org/10.1016/j.neucom.2022.04.091>.
- [123] Bassett DS, Wymbs NF, Porter MA, Mucha PJ, Carlson JM, Grafton ST. Dynamic reconfiguration of human brain networks during learning. *Proc. Natl. Acad. Sci.* 2011;108:7641–6. <https://doi.org/10.1073/pnas.1018985108>.
- [124] Finc K, Bonna K, He X, Lydon-Staley DM, Kühn S, Duch W, Bassett DS. Dynamic reconfiguration of functional brain networks during working memory training. *Nat Commun* 2020;11:2435. <https://doi.org/10.1038/s41467-020-15631-z>.
- [125] Geib BR, Stanley ML, Wing EA, Laurienti PJ, Cabeza R. Hippocampal Contributions to the Large-Scale Episodic Memory Network Predict Vivid Visual Memories. *Cereb. Cortex* 2017;27:680–93. <https://doi.org/10.1093/cercor/bhv272>.
- [126] Vaiana M, Muldoon SF. Multilayer Brain Networks. *J. Nonlinear Sci.* 2020;30:2147–69. <https://doi.org/10.1007/s00332-017-9436-8>.
- [127] Battiston F, Nicosia V, Chavez M, Latora V. Multilayer motif analysis of brain networks. *Chaos Interdiscip. J. Nonlinear Sci.* 2017;27:047404. <https://doi.org/10.1063/1.4979282>.
- [128] Birn RM. The role of physiological noise in resting-state functional connectivity. *NeuroImage*. 20 YEARS OF fMRI 2012;62:864–70. <https://doi.org/10.1016/j.neuroimage.2012.01.016>.
- [129] Power JD, Barnes KA, Snyder AZ, Schlaggar BL, Petersen SE. Spurious but systematic correlations in functional connectivity MRI networks arise from subject motion. *NeuroImage* 2012;59:2142–54. <https://doi.org/10.1016/j.neuroimage.2011.10.018>.
- [130] Cole MW, Ito T, Schultz D, Mill R, Chen R, Cocuzza C. Task activations produce spurious but systematic inflation of task functional connectivity estimates. *NeuroImage* 2019;189:1–18. <https://doi.org/10.1016/j.neuroimage.2018.12.054>.
- [131] Birn RM, Diamond JB, Smith MA, Bandettini PA. Separating respiratory-variation-related fluctuations from neuronal-activity-related fluctuations in fMRI. *NeuroImage* 2006;31:1536–48. <https://doi.org/10.1016/j.neuroimage.2006.02.048>.
- [132] Power JD, Mitra A, Laumann TO, Snyder AZ, Schlaggar BL, Petersen SE. Methods to detect, characterize, and remove motion artifact in resting state fMRI. *NeuroImage* 2014;84:320–41. <https://doi.org/10.1016/j.neuroimage.2013.08.048>.
- [133] Power JD, Plitt M, Gotts SJ, Kundu P, Voon V, Bandettini PA, Martin A. Ridding fMRI data of motion-related influences: Removal of signals with distinct spatial and physical bases in multiecho data. *Proc. Natl. Acad. Sci.* 2018;115:E2105–14. <https://doi.org/10.1073/pnas.1720985115>.
- [134] Spreng RN, Fernández-Cabello S, Turner GR, Stevens WD. Take a deep breath: Multiecho fMRI denoising effectively removes head motion artifacts, obviating the need for global signal regression. *Proc. Natl. Acad. Sci.* 2019;116:19241–2. <https://doi.org/10.1073/pnas.1909848116>.
- [135] Power JD, Lynch CJ, Gilmore AW, Gotts SJ, Martin A. Reply to Spreng et al.: Multiecho fMRI denoising does not remove global motion-associated respiratory signals. *Proc. Natl. Acad. Sci.* 2019;116:19243. <https://doi.org/10.1073/pnas.1909852116>.
- [136] Havlicek M, Friston KJ, Jan J, Brazdil M, Calhoun VD. Dynamic modeling of neuronal responses in fMRI using cubature Kalman filtering. *NeuroImage* 2011;56:2109–28. <https://doi.org/10.1016/j.neuroimage.2011.03.005>.
- [137] Ngo GC, Holtrop JL, Fu M, Lam F, Sutton BP. High temporal resolution functional MRI with partial separability model. In: 2015 37th Annual International Conference of the IEEE Engineering in Medicine and Biology Society (EMBC). Presented at the 2015 37th Annual International Conference of the IEEE Engineering in Medicine and Biology Society (EMBC); 2015. p. 7482–5. <https://doi.org/10.1109/EMBC.2015.7320122>.
- [138] Friston KJ, Moran R, Seth AK. Analysing connectivity with Granger causality and dynamic causal modelling. *Curr. Opin. Neurobiol.*, *Macrocircuits* 2013;23:172–8. <https://doi.org/10.1016/j.conb.2012.11.010>.
- [139] Lurie DJ, Kessler D, Bassett DS, Betzel RF, Breakspear M, Kheilholz S, Kucyi A, Liégeois R, Lindquist MA, McIntosh AR, Poldrack RA, Shine JM, Thompson WH, Bielczyk NZ, Douw L, Kraft D, Miller RL, Muthuraman M, Pasquini L, Razi A, Vidaurri D, Xie H, Calhoun VD. Questions and controversies in the study of time-varying functional connectivity in resting fMRI. *Netw. Neurosci* 2020;4:30–69. [https://doi.org/10.1162/netn\\_a.00116](https://doi.org/10.1162/netn_a.00116).
- [140] Penny WD, Stephan KE, Mechelli A, Friston KJ. Modelling functional integration: a comparison of structural equation and dynamic causal models. *NeuroImage*, *Mathematics in Brain Imaging* 2004;23:S264–74. <https://doi.org/10.1016/j.neuroimage.2004.07.041>.
- [141] Motlaghian SM, Belger A, Bustillo JR, Ford JM, Iraji A, Lim K, Mathalon DH, Mueller BA, O’Leary D, Pearlson G, Potkin SG, Preda A, van Erp TGM, Calhoun VD. Nonlinear functional network connectivity in resting functional magnetic resonance imaging data. *Hum Brain Mapp* 2022;43:4556–66. <https://doi.org/10.1002/hbm.25972>.
- [142] Su L, Wang L, Shen H, Feng G, Hu D. Discriminative analysis of non-linear brain connectivity in schizophrenia: an fMRI Study. *Front Hum Neurosci* 2013;7.
- [143] Xie X, Cao Z, Weng X. Spatiotemporal nonlinearity in resting-state fMRI of the human brain. *NeuroImage* 2008;40:1672–85. <https://doi.org/10.1016/j.neuroimage.2008.01.007>.
- [144] Hlinka J, Paluš M, Vejmelka M, Mantini D, Corbetta M. Functional connectivity in resting-state fMRI: Is linear correlation sufficient? *NeuroImage* 2011;54:2218–25. <https://doi.org/10.1016/j.neuroimage.2010.08.042>.
- [145] Poskanzer C, Fang M, Aglinskas A, Anzellotti S. Controlling for Spurious Nonlinear Dependence in Connectivity Analyses. *Neuroinformatics* 2022;20:599–611. <https://doi.org/10.1007/s12021-021-09540-9>.
- [146] Ahmadadi H, Fatemizadeh E, Motie Nasrabad A. A Comparative Study of Correlation Methods in Functional Connectivity Analysis Using fMRI Data of Alzheimer’s Patients. *J. Biomed. Phys. Eng.* 2023;13:125–34. <https://doi.org/10.31661/jbpe.v0i0.2007-1134>.
- [147] Poskanzer C, Anzellotti S. Functional coordinates: Modeling interactions between brain regions as points in a function space. *Netw. Neurosci* 2022;6:1296–315. [https://doi.org/10.1162/netn\\_a.00264](https://doi.org/10.1162/netn_a.00264).
- [148] Hastie T, Tibshirani R. *Generalized Additive Models. Stat Sci* 1986;1:297–310.
- [149] Sóskuthy, M., 2017. Generalised additive mixed models for dynamic analysis in linguistics: a practical introduction. <https://doi.org/10.48550/arXiv.1703.05339>.
- [150] Kvålsseth TO. On Normalized Mutual Information: Measure Derivations and Properties. *Entropy* 2017;19:631. <https://doi.org/10.3390/e19110631>.
- [151] Shannon CE. A mathematical theory of communication. *Bell Syst. Tech. J.* 1948;27:379–423. <https://doi.org/10.1002/j.1538-7305.1948.tb01338.x>.
- [152] Arabie P, Boorman SA. Multidimensional scaling of measures of distance between partitions. *J Math Psychol* 1973;10:148–203. [https://doi.org/10.1016/0022-2496\(73\)90012-6](https://doi.org/10.1016/0022-2496(73)90012-6).
- [153] Geerligs L, Cam-CAN, Henson RN. Functional connectivity and structural covariance between regions of interest can be measured more accurately using multivariate distance correlation. *NeuroImage* 2016;135:16–31. <https://doi.org/10.1016/j.neuroimage.2016.04.047>.
- [154] Székely GJ, Rizzo ML, Bakirov NK. Measuring and testing dependence by correlation of distances. *Ann Stat* 2007;35:2769–94. <https://doi.org/10.1214/090536070000000505>.
- [155] Marwan N, Carmen Romano M, Thiel M, Kurths J. Recurrence plots for the analysis of complex systems. *Phys Rep* 2007;438:237–329. <https://doi.org/10.1016/j.physrep.2006.11.001>.

- [156] Marwan N, Kurths J. Nonlinear analysis of bivariate data with cross recurrence plots. *Phys Lett A* 2002;302:299–307. [https://doi.org/10.1016/S0375-9601\(02\)01170-2](https://doi.org/10.1016/S0375-9601(02)01170-2).
- [157] Kashyap A, Keilholz S. Dynamic properties of simulated brain network models and empirical resting-state data. *Netw Neurosci* 2019;3:405–26. [https://doi.org/10.1162/netn\\_a\\_00070](https://doi.org/10.1162/netn_a_00070).
- [158] Lopes MA, Zhang J, Krzemieński D, Hamandi K, Chen Q, Livi L, Masuda N. Recurrence quantification analysis of dynamic brain networks. *Eur J Neurosci* 2021;53:1040–59. <https://doi.org/10.1111/ejn.14960>.
- [159] Yargholi E, Hosseini-Zadeh GA. Cross recurrence quantifiers as new connectivity measures for structure learning of Bayesian networks in brain decoding. *Chaos Solitons Fractals* 2019;123:263–74. <https://doi.org/10.1016/j.chaos.2019.04.019>.
- [160] Simony E, Honey CJ, Chen J, Lositsky O, Yeshurun Y, Wiesel A, Hasson U. Dynamic reconfiguration of the default mode network during narrative comprehension. *Nat Commun* 2016;7:12141. <https://doi.org/10.1038/ncomms12141>.
- [161] Kim D, Kay K, Shulman GL, Corbetta M. A New Modular Brain Organization of the BOLD Signal during Natural Vision. *Cereb. Cortex* 2018;28:3065–81. <https://doi.org/10.1093/cercor/bhx175>.
- [162] Xie H, Redcay E. A tale of two connectivities: intra- and inter-subject functional connectivity jointly enable better prediction of social abilities. *Front Neurosci* 2022;16.